ChemMedChem

Research Article
doi.org/10.1002/cmdc.202300322

Chemistry Europe
European Chemical Societies Publishing

www.chemmedchem.org

Design and Synthesis of Novel 2-Acetamido, 6-Carboxamide Substituted Benzothiazoles as Potential BRAFV600E Inhibitors – *In vitro* Evaluation of their Antiproliferative Activity

Yakinthi Batsi,[a] Georgia Antonopoulou,[a] Theano Fotopoulou,[a] Kassandra Koumaki,[a] Eftichia Kritsi,[a] Constantinos Potamitis,[a] Maria Goulielmaki,[a] Salomi Skarmalioraki,[a] Chara Papalouka,[a] Eleni Poulou-Sidiropoulou,[a] Vivian Kosmidou,[a] Stavroula Douna,[a] Maria-Sofia Vidali,[a] Eleni-Fani Gkotsi,[a] Aristotelis Chatziioannou,[a] Vassilis L. Souliotis,[a] Vasiliki Pletsa,[a] Olga Papadodima,[a] Vassilis Zoumpourlis,[a] Panagiotis Georgiadis,[a] Maria Zervou,[a] Alexander Pintzas,[a] and Ioannis D. Kostas*[a]

The oncogenic BRAFV600E kinase leads to abnormal activation of the MAPK signaling pathway and thus, uncontrolled cellular proliferation and cancer development. Based on our previous virtual screening studies which issued 2-acetamido-1,3 benzothiazole-6-carboxamide scaffold as active pharmacophore displaying selectivity against the mutated BRAF, eleven new substituted benzothiazole derivatives were designed and synthesized by coupling of 2-acetamidobenzo[d]thiazole-6-carboxylic acid with the appropriate amines in an effort to provide even more efficient inhibitors and tackle drug resistance often developed during cancer treatment. All derived compounds bore the benzothiazole scaffold substituted at position-2 by an acetamido moiety and at position-6 by a carboxamide functionality, the NH moiety of which was further linked through an alkylene linker to a sulfonamido (or amino) aryl (or alkyl) functionality or a phenylene linker to a sulfonamido aromatic (or non-aromatic) terminal pharmacophore in the order $-C_6H_4-NHSO_2-R$ or reversely $-C_6H_4-SO_2N(H)-R$. These analogs were subsequently biologically evaluated as potential BRAFV600E inhibitors and antiproliferative agents in several colorectal cancer and melanoma cell lines. In all assays applied, one analog, namely 2-acetamido-*N*-[3-(pyridin-2-ylamino)propyl]benzo[d]thiazole-6-carboxamide (**22**), provided promising results in view of its use in drug development.

Introduction

The RAF kinases are serine/threonine-specific protein kinases, consisting of three members: ARAF, BRAF and CRAF.[1,2] This family of protein kinases plays critical role in the RAS-RAF-MEK-ERK MAPK pathway, an important signaling cascade that regulates critical cellular mechanisms, such as proliferation and survival.[3,4] Specifically, RAF proteins act as a central link between the membrane-bound RAS GTPases and the downstream kinases MEK and ERK.[5,6] ERK activation promotes cellular growth and differentiation, resulting in oncogenesis.[7] Thus, the MAPK pathway is linked to oncogenic mutations that are observed in many cancers.[8]

BRAF was the last member of the RAF family discovered in 1988.[2,8] In 2002, BRAF was identified as a driver oncogene by the Cancer Genome project and since then, more than 45 oncogenic mutations have been described for BRAF.[1,8] The majority of BRAF mutations (~90%) consist of a glutamic acid substitution of the valine at position 600 (V600E) within the activation segment of the kinase.[1,9] Overall, BRAF mutations are present in about 8% of human tumors.[8,10] BRAF mutations occur in ~50% of patients with melanoma, 25–45% in thyroid carcinomas, in 5–10% of colorectal cancer patients, almost 100% in hairy cell leukemia cases and less commonly in ovarian and lung malignancies.[8,11] The mutated BRAFV600E overcomes the need for extracellular stimuli, allowing the kinase to perform a ~500 fold increase in catalytic activity compared to the wild type, leading to abnormal activation of the MAPK signaling pathway. As a result, MEK and ERK are phosphorylated constantly leading to uncontrolled cellular proliferation and survival activities and thus cancer development.[2,4,7]

In previous years, numerous BRAF inhibitors have been developed targeting oncogenic BRAFV600E.[7] FDA has approved two inhibitors (Vemurafenib in 2011 and Dabrafenib in 2013) for the treatment of BRAF mutant melanoma patients in

[a] *Y. Batsi, Dr. G. Antonopoulou, Dr. T. Fotopoulou, K. Koumaki, Dr. E. Kritsi, Dr. C. Potamitis, Dr. M. Goulielmaki, S. Skarmalioraki, C. Papalouka, E. Poulou-Sidiropoulou, V. Kosmidou, S. Douna, M.-S. Vidali, E.-F. Gkotsi, Dr. A. Chatziioannou, Dr. V. L. Souliotis, Dr. V. Pletsa, Dr. O. Papadodima, Dr. V. Zoumpourlis, Dr. P. Georgiadis, Dr. M. Zervou, Dr. A. Pintzas, Dr. I. D. Kostas*
Institute of Chemical Biology
National Hellenic Research Foundation
Vas. Constantinou Ave. 48, 11635 Athens (Greece)
E-mail: ikostas@eie.gr

Supporting information for this article is available on the WWW under https://doi.org/10.1002/cmdc.202300322

an advanced stage.[8,12,13] Both Vemurafenib and Dabrafenib have demonstrated clinical benefits performing response rates of 50% and improving the survival of melanoma patients with BRAFV600 mutant tumors.[8,13] However, these drugs paradoxically activate the MAPK pathway, promoting the dimerization of wild-type B-Raf and C-Raf in cell lines expressing Ras mutants.[5] Also, therapy comes along with adverse effects like the development of secondary cancers, such as cutaneous squamous cell carcinomas and keratoacanthomas.[9,14] Moreover, resistance is acquired limiting their effectiveness and most patients relapse within a year.[8] About 50% of the patients do not respond to therapy, while only 5% of patients with colorectal cancer harboring BRAFV600E mutation respond and even in that case, the prognosis is usually poor.[1,10,13]

In order to improve response and to overcome resistance, combination therapy of BRAF and MEK inhibitors was suggested.[15,16] Currently, there are three combinations approved by the FDA: Vemurafenib with Cobimetinib (MEKi), Dabrafenib with Trametinib (MEKi) and Encorafenib (BRAFi) with Binimetinib (MEKi). All combinations are effective showing response rates of more than 63%.[17,18,19,20] Although combination therapy improves overall survival, all patients affected with melanoma will develop a tumor within a year, so resistance still develops.[21,22] Some other combinatorial treatments of BRAF targeting drugs with inhibitors of the MAPK pathway were examined and recently, FDA approved Atezolizumab (PD–L1) in combination with Cobimetinib and Vemurafenib for patients with BRAFV600 mutation-positive unresectable or metastatic melanoma and also Encorafenib in combination with Cetuximab (EGFRi) for metastatic colorectal cancer with a BRAFV600E mutation.[23]

All the above challenges in the treatment of tumors with BRAF inhibitors led to the development of two next-generation RAF inhibitors that do not exhibit paradoxical ERK activation, **PLX7904** and **PLX8394** (Figure 1). These compounds show a potency against mutant BRAF similar to Vemurafenib but do not drive RAF dimerization.[14] **PLX8394** selectively disrupts BRAF homo- and BRAF–CRAF heterodimers but is ineffective against CRAF homodimers.[24,25] The "paradox breakers" are predicted to show decreased toxicity and afford a wide therapeutic window. The structural and chemical principles of these drugs can lead to the design of new RAF inhibitors with improved biological profiles and bring us one step closer to targeting BRAF mutations in human cancers efficiently.[14,25]

In the present work, we report the design and synthesis of eleven new substituted benzothiazole derivatives by coupling of a 2,6-substituted benzothiazole carboxylic acid with the appropriate amines. *In vitro* biological evaluation of these molecules as potential BRAFV600E inhibitors in several cancer cell lines provided promising results.

Results and Discussion

In silico studies and BRAFV600E inhibition

A series of compounds were designed based on the 1,3 benzothiazole–amide scaffold which emerged as active pharmacophore against BRAFV600E through a previous pharmacophore-based Virtual Screening study using the crystal complex BRAFV600E: Vemurafenib (unpublished data). In the current study we followed a structure-based optimization approach using the crystal structure of BRAFV600E complexed with the paradox breaker **PLX7904** (PDB: 4XV1).

We followed a two-fold strategy seeking to succeed in new synthetic analogs with increased specific activity against BRAFV600E compared to the wtBRAF. All derived compounds bore the benzothiazole scaffold substituted at positions-2 and 6 by carboxamide functionalities with the functionality at position-2 being an acetamido moiety (Figure 2). The NH moiety of the carboxamide at position-6 was further linked through an alkylene linker to a sulfonamido aromatic or alkyl terminal pharmacophore (analogs **20** and **21**, respectively) or to an amine aromatic terminal functionality (analogs **22** and **23**). Our second strategy functionalized the NH of the carboxamide at position-6 with a phenylene linker attached to sulfonamido aromatic (or non-aromatic) terminal pharmacophore (analogs **24**–**30**).

The predicted ADME properties of the compounds were satisfactory, displaying values within the 95% range of the known drugs (Table S1, Supporting Information).

Analogs with alkylene linker

In silico docking at the active site of the mutated protein as retained from its complex with the paradox breaker **PLX7904** revealed that the mother compound of this series **20** was

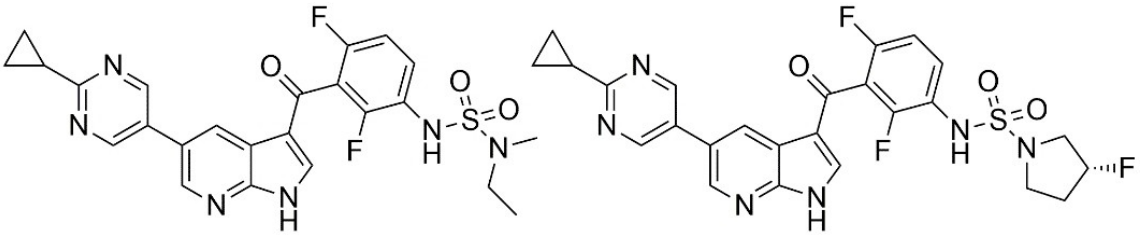

Figure 1. Chemical structures of **PLX7904** and **PLX8394** with a potency against mutant BRAF.

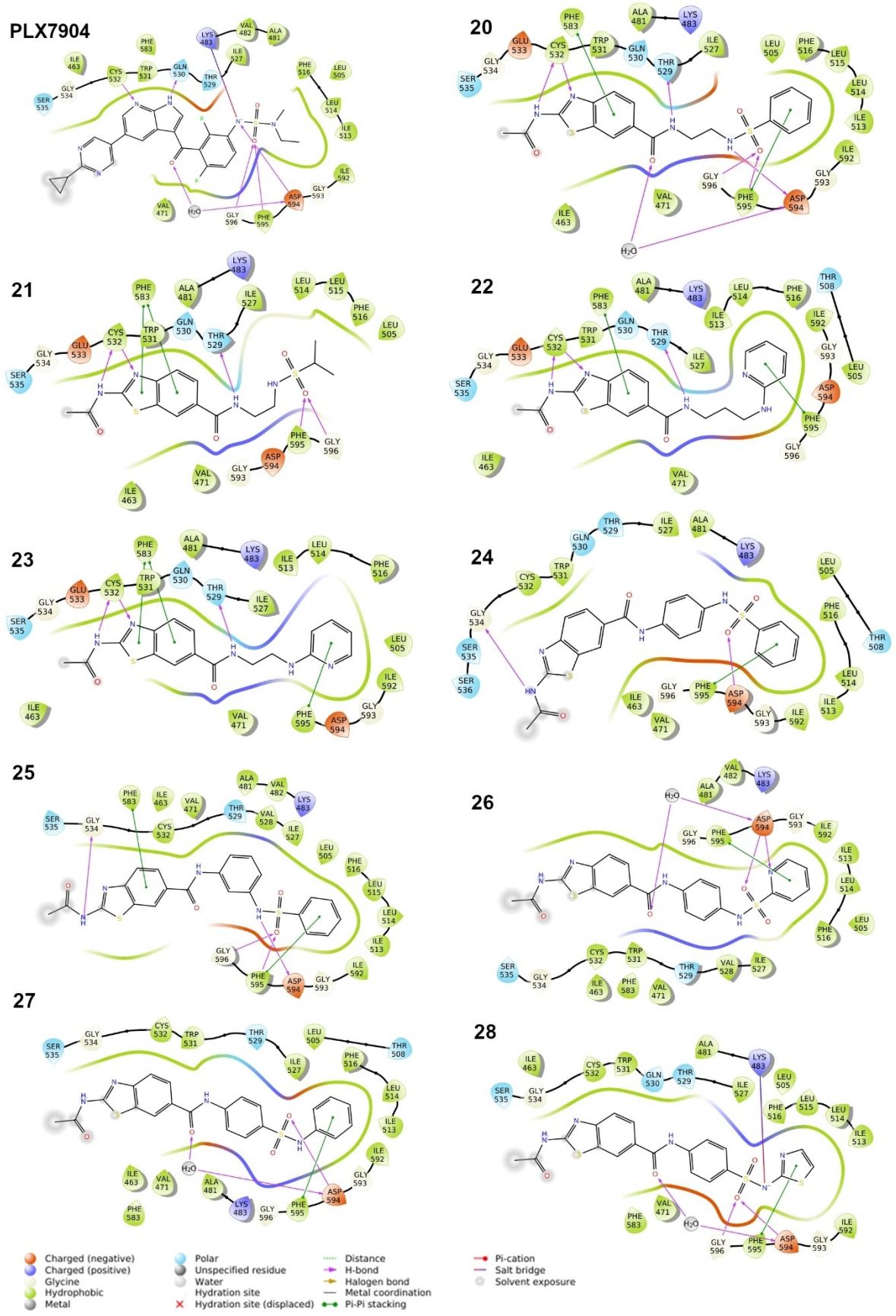

Figure 2. *In silico* docking of the studied analogs at the catalytic site of BRAFV600E (pdb: 4XV1); 2D ligand interaction diagrams of the proposed binding poses. The paradox breaker **PLX7904** as retained from the crystal complex is also presented for comparison.

capable of maintaining the majority of the crucial interactions (Figures 2 & 3). The benzothiazole is accommodated within the adenine-binding region of the ATP pocket, surrounded by residues Cys532, Trp531, Gln530, Phe583. Compound **20** uses the thiazole N3 and the adjacent NH to contact the hinge region through two H-bonds with Cys532 while enables additionally a π-π interaction between the benzene ring and Phe583 (C lobe). The NH moiety of the carboxamide at position-6 of the benzothiazole is oriented towards the same space as the benzene fluorine of **PLX7904** and may successfully contact the gatekeeper amino acid Thr529 while the CO moiety mimics the corresponding group of the drug and bridges the interaction with the critical Asp594 of the DFG motif *via* the conserved water.

The ethylene linker of **20** aids in the proper orientation of the sulfonamide pharmacophore in order to contact directly through H-bonds the crucial DFG amino acids (Phe595, the catalytic Asp594 and Gly596) mimicking the corresponding contacts of **PLX7904**. Moreover, the terminal aromatic ring of **20** also enables additionally a π-π interaction with Phe595 stabilizing further the binding. Compound **20** presented a concentration-dependent inhibition with specificity against BRAFV600E as presented in the Table 1 ($IC_{50} = 21.3\ \mu M$).

We observed a lipophilic pocket formed by the amino acids Leu505, Phe516, Leu515, Leu514, Ile513, Ile592, which favors the hosting of the terminal aromaticity. In line with this, the substitution of the terminal aromatic ring with an isopropyl moiety leads to loss of activity as observed for analog **21**, although the analog retained the interactions with the adenine pocket and developed direct contacts with amino acids of the DFG motif (Phe595, Gly596). This triggered us to retain the terminal aromaticity throughout the following study.

Subsequently, we eliminated the sulfo group and linked the amine directly to a pyridine terminal functionality as in analog **23**. Although displaying less contacts with the DFG motif, this configuration succeeded in regaining the concentration-dependent inhibition also displaying selectivity against the mutated protein. The extension of the alkylene linker by one carbon atom as in **22** increases the ligand efficiency resulting in the most active compound ($IC_{50} = 7.87\ \mu M$). Besides retaining the critical interactions with adenine binding pocket, compound **22** smoothly accommodates the terminal pyridine in the lipophilic pocket (Ile513, Leu514 and Phe516 of β4 sheet following aC-helix, N-lobe) and is surrounded also by Ile592, Gly593 (activation loop) and the following triad of the DFG motif while a π-π interaction with Phe595 further stabilizes the binding (Figures 2 & 3).

The above-mentioned results showed that the benzothiazole scaffold substituted at position-6 by a second carboxamide functionality emerges as a promising scaffold against BRAFV600E. An ethylene-linker towards the sulfonamide–benzyl final functionality (as in analog **20**) or propylene-linker towards the amine–pyridine tail (as in analog **22**), are well tolerated and critical contacts with the DFG region are retained. Although both compounds display lower inhibition against BRAFV600E as compared to the drug Vemurafenib, they display notable selectivity against wtBRAF (Table 1).

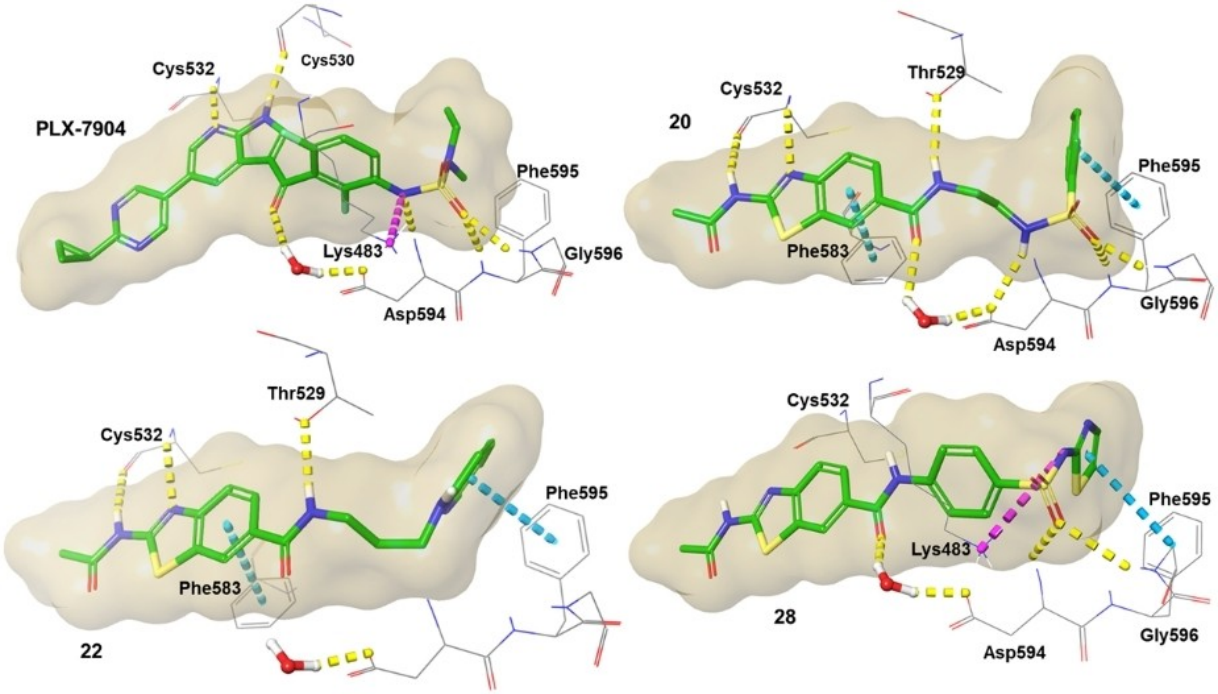

Figure 3. 3D representation of the binding modes of the most active compounds **20**, **22** and **28** at the catalytic site of BRAFV600E (pdb: 4XV1). The paradox breaker **PLX7904** as retained from the crystal complex is also presented for comparison.

Table 1. *In silico* docking score at the paradox breaker complex with BRAFV600E and *in vitro* cell-free kinase assay inhibition against BRAFV600E and wtBRAF.

Compound	XP docking score [kcal·mol^{-1}]	BRAFV600E inhibition[a,b]			wtBRAF inhibition[a,b]	
		% inhibition at 10 μM	% inhibition at 100 μM	IC_{50} [μM][c]	% inhibition at 10 μM	% inhibition at 100 μM
20	−12.50	44	84	21.3	21	50
21	−10.71	22	11	n.d.	18	8
22	−11.39	45	79	7.87	−2	35
23	−10.11	19	62	n.d.	−2	39
24	−6.79	5	6	n.d.	4	5
25	−7.75	12	50	n.d.	−10	12
26	−7.90	13	13	n.d.	−15	−6
27	−7.35	36	32	n.d.	4	4
28	−6.64	47	69	n.d.	−9	38
29	−4.96	0	11	n.d.	0	2
30	−5.07	3	20	n.d.	1	21
PLX7904	−12.26	n.d.	n.d.	n.d.	n.d.	n.d.

[a] ATP [μM] = 100 optimized against the known inhibitor Staurosporine as determined by SelectScreen™ Screening Protocol and Assay Conditions; [b] For comparison reasons, the inhibition constants of the drug Vemurafenib have been also determined against BRAFV600E (% inhibition at 100 μM = 95 and at 10 μM = 94) and against wtBRAF (% inhibition at 100 μM = 96 and at 10 μM = 94); [c] IC_{50} was determined for the most active compounds; n.d. = not determined.

Analogs with phenylene linker

Having established the critical role of the tail aromaticity, our second strategy involved the reduction of the ligand flexibility through replacing the alkylene linker by phenylene further substituted by the critical sulfonamide pharmacophore. The analog **25** featuring a *meta*-substitution of the phenylene linker retains the crucial interactions with the DFG region attributed to the presence of the sulfonamide (three H-bonds with Gly596, Phe595 and the catalytic Asp594), but also to the favorable hosting of the terminal benzene which additionally interacts through π-π with Phe595. On the other hand, the imposed restriction of flexibility shifts the carboxy–benzothiazole towards the solvent disfavoring the contact with Cys532 although the NH substitution at position-6 develops H-bonding with Gly534 of the hinge region (Figure 2). The unfavorable binding is also mirrored in the reduced activity at the kinase assay (Table 1). The *para*-substitution of the phenylene linker as in **24** was not effective. However, further replacement of the terminal benzene with pyridine as in **26** improved the binding interactions with the DFG region (two H-bonds with the catalytic Asp594 and π-π interaction with Phe595) and re-established the water bridging of the carboxyl moiety with Asp594. Despite that, the analog cannot successfully contact the hinge region and further stabilize its binding. We subsequently tested the inversion of the sulfonamide group as in **27**, but this was not effective towards a concentration-dependent inhibition.

Interestingly though, the analog **28** which features sulfonamide inversion with charged nitrogen as in the drug and a thiazole terminal pharmacophore successfully reproduces the critical interactions with the DFG region (direct and indirect H-bonding with Asp594, H-bond with Gly596 and π-π interaction with Phe595) while additionally the presence of the charged N atom emerges critical in establishing the ionic interaction with the catalytic Lys483 mimicking the drug (Figures 2 & 3). Although, *in silico* studies show that **28** is not capable to contact the hinge region with its benzothiazole pharmacophore, results of the kinase assay point to a concentration dependent inhibition with selectivity against BRAFV600E displaying similar potency as the more potent compound **22** (Table 1). Lastly, our SAR studies also involved a terminal morpholine or piperidine ring directly linked to the sulfo group (analogs **29** and **30**, respectively), resulting in loss of activity as no interactions with the DFG region can be stabilized (docking poses not shown).

In summary, the restriction of ligand flexibility by replacing the alkylene linker by phenylene disfavors the critical contacts of the carboxy–benzothiazole with the hinge region. Inversion of the sulfonamide and the presence of charged nitrogen restores the activity of this class of compounds mainly through the contacts with the DFG region.

Chemical synthesis

As mentioned in the Introduction, the synthesis of the target molecules was achieved by coupling of a 2,6-substituted benzothiazole carboxylic acid with the appropriate amines. The preparation of 2-acetamidobenzo[d]thiazole-6-carboxylic acid (**6**) and the appropriate references are illustrated in Scheme 1. Esterification of the carboxylic group of 4-nitrobenzoic acid (**1**) led to compound **2**,[26] the nitro group of which was reduced by $SnCl_2$ in ethanol under ultrasound irradiation to afford the

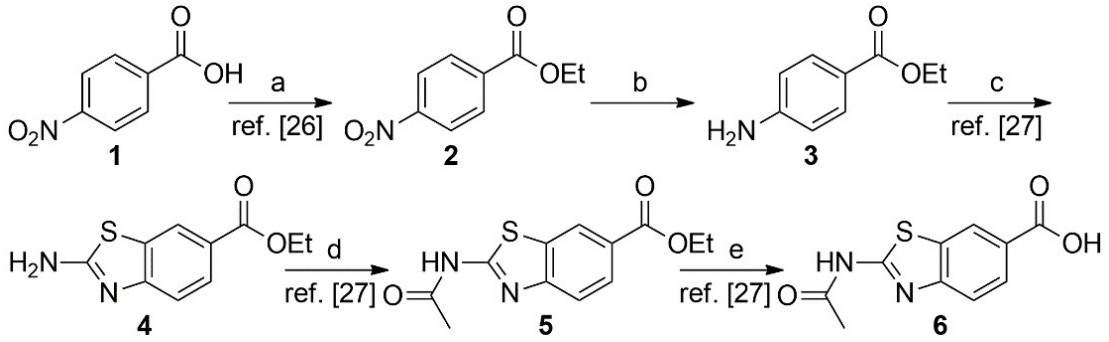

Scheme 1. Synthetic sequence for the preparation of 2-acetamidobenzo[d]thiazole-6-carboxylic acid (**6**). *Reagents and conditions:* (a) EtOH, H_2SO_4, 75 °C, 8 h, 92%; (b) $SnCl_2$, EtOH, ultrasound irradiation, 50 °C, 40 kHz, 1 h, 85%; (c) AcOH, KSCN, Br_2, r.t., 68%; (d) Ac_2O, 80 °C, 6 h, 78%; (e) 1 M NaOH, MeOH, r.t., 4 h and then 1 M HCl, 98%.

amino derivative **3**. Subsequently, treatment of **3** with KSCN and Br_2 in acetic acid led to the benzothiazole derivative **4**.[27] Finally, acetylation of the amine group followed by hydrolysis of the ester group of **5** yielded the carboxylic acid **6**.[27] It should pointed out that the cited references for compounds **2**, **4**, **5** and **6** do not include any NMR data for these molecules. Further details and other references for the preparation of compounds **2**–**6** by other procedures, including NMR data (if appropriate), are given in the Supporting Information (SI).

The amines **9a**–**k** used for the coupling with acid **6** were prepared as shown in Schemes 2–4. Scheme 2 includes amines with ethylene or propylene linker between the primary amino group (NH_2) and the sulfonamido (or amino) alkyl or aryl functionality, while Schemes 3 and 4 involve the analogs with a phenylene linker. In several synthetic steps, we used the same or modified procedures described in the cited references for the same compounds, despite the fact that some of them were previously characterized by spectral data. Further details and other references for the preparation of these compounds are given in SI.

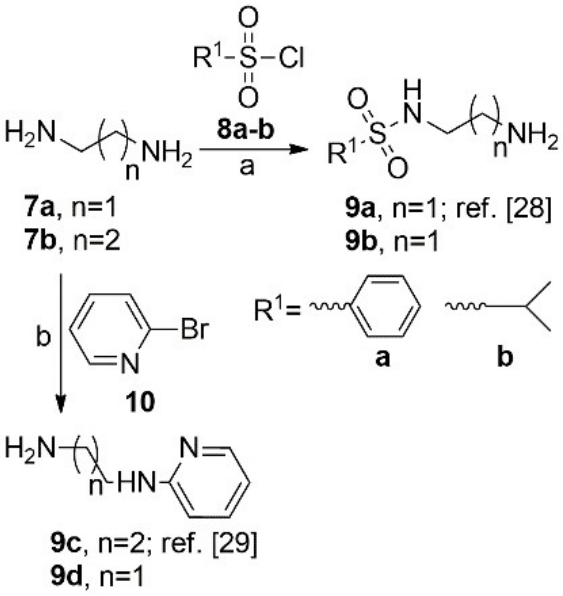

Scheme 2. Synthesis of amines **9a**–**d** with an alkylene linker. *Reagents and conditions:* (a) CH_2Cl_2, r.t., 30 min, 68–70%; (b) Pyridine, reflux, 22–48 h, 46–65%.

For the preparation of the amines **9a**[28] and **9b**, ethylenediamine (**7a**) was treated with the appropriate sulfonyl chloride **8a** or **8b**, respectively, while for the synthesis of the amines **9c**[29] and **9d**, 1,3-diaminopropane (**7b**) or ethylenediamine (**7a**), respectively, was treated with 2-bromopyridine (**10**) (Scheme 2).

Synthesis of the amines **9e** and **9f**[30] was achieved in one step by the reaction of benzenesulfonyl chloride (**8a**) with *p*-phenylenediamine (**11**) or *m*-phenylenediamine (**12**), respectively (Scheme 3). The amine **9g** was synthesized in a two-step procedure by coupling of the Boc-protected amine **13**[31] (prepared from *p*-phenylenediamine (**11**)) and the sulfonyl chloride **15**[32] (prepared by oxidation of 2-mercaptopyridine (**14**)), followed by deprotection of the Boc moiety with trifluoroacetic acid (TFA).

Scheme 4 describes the preparation of amines **9h**–**k** with the phenylene linker connected to the sulfonamido moiety in the order $–C_6H_4–SO_2N(H)–R$, which is the reverse order compared to amines **9e**–**g**. They have been prepared by coupling of 4-nitro-benzenesulfonyl chloride (**17**) with the appropriate amines **18a**–**d** in the presence of a base to afford the nitro derivatives **19a**–**d**,[33–36] followed by reduction of the nitro to the amino group using iron powder and ammonium chloride solution in ethanol for amines **9i** and **9j** or alternatively, $SnCl_2$ in ethanol under ultrasound irradiation for amines **9h** and **9k**.

Finally, coupling of 2-acetamidobenzo[d]thiazole-6-carboxylic acid (**6**) with the amines **9a**–**k** afforded the target 2-acetamido, 6-carboxamide substituted benzothiazole derivatives **20**–**30** (Scheme 5, Figure 4). We used different coupling agents: (a) *N*-ethoxycarbonyl-2-ethoxy-1,2-dihydroquinoline (EEDQ); (b) 1-ethyl-3-(3-dimethylaminopropyl)carbodiimide (EDC), 4-(dimethylamino)pyridine (DMAP) or 1-hydroxybenzotriazole (HOBt).

All new compounds were fully characterized by NMR and high resolution mass spectrometry (HRMS), in which the measured accurate masses corresponded exactly to the proposed formulas. In the ^{1}H NMR spectra of all final products, the

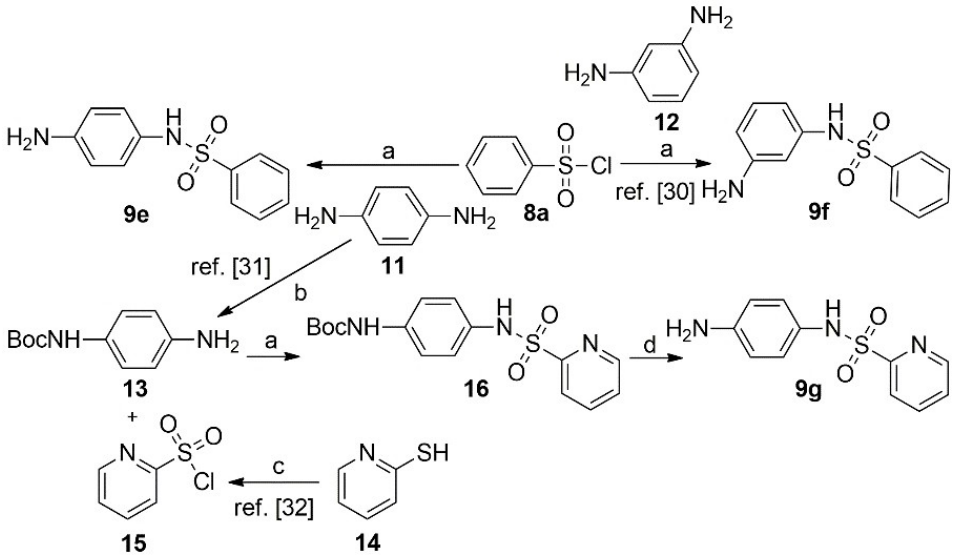

Scheme 3. Synthesis of amines **9e–g** with a phenylene linker in the order $-C_6H_4-NHSO_2-R$. *Reagents and conditions:* (a) Et_3N, THF, 0 °C to r.t., 2.5–18 h, 30–40%; (b) Boc anhydride, CH_2Cl_2, 0 °C to r.t., 16 h, 46%; (c) H_2SO_4, aq. $NaClO_4$ 5%, 0 °C, 30 min, 99%; (d) TFA, CH_2Cl_2, 0 °C to r.t., 1 h and 40 min, 75%.

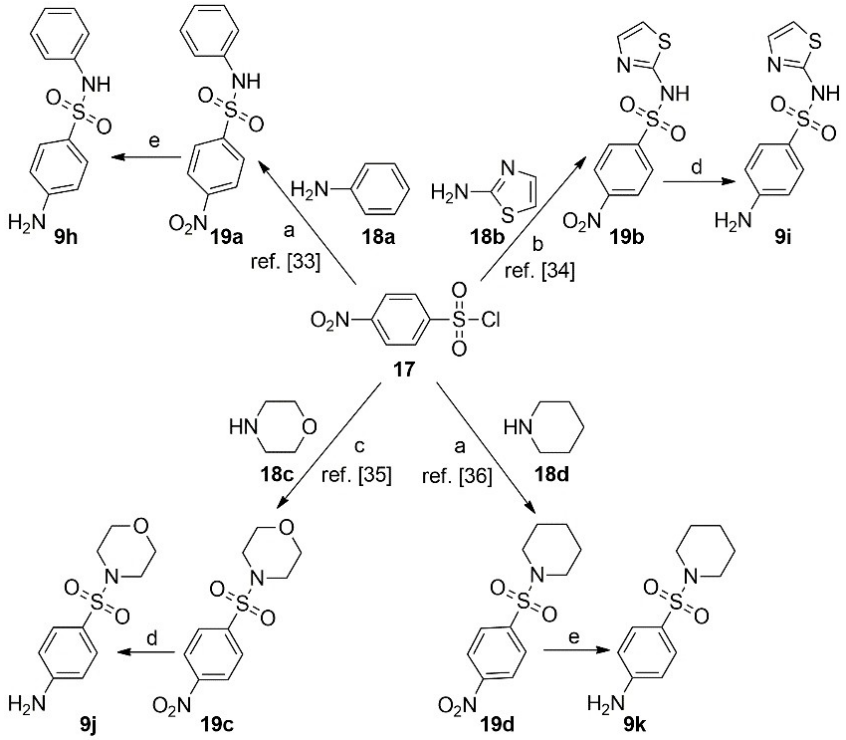

Scheme 4. Synthesis of amines **9h–k** with a phenylene linker in the order $-C_6H_4-SO_2N(H)-R$. *Reagents and conditions:* (a) pyridine, CH_2Cl_2, r.t., 2–18 h, 60–80%; (b) pyridine, 0 °C to r.t., 18 h, 61%; (c) Et_3N, CH_2Cl_2, 0 °C to r.t., 3 h, 100%; (d) Fe powder, aq. NH_4Cl, EtOH, reflux 3–3.5 h, 80–100%; (e) $SnCl_2$, EtOH, US irradiation, 50 °C, 40 kHz, 1 h, 87–100%.

NH proton of the acetamido functionality at position-2 of the benzothiazole scaffold is shifted to ~12.5 ppm. On the other hand, the NH proton of the carboxamide functionality at position-6 is shifted to ~12.5 ppm in the case that the NH moiety is attached to an alkylene linker (**20**, **21**, **22** and **23**) or to ~10.2 ppm when it is attached to a phenylene linker connected with the sulfonamido moiety in the order $-C_6H_4-NHSO_2-R$ (**24**, **25** and **26**), being ~10.7 ppm in the case of the reverse order $-C_6H_4-SO_2N(H)-R$ (**27**, **28**, **29** and **30**). The purity of the tested compounds was over 96% as indicated by high-performance liquid chromatography (HPLC) analysis.

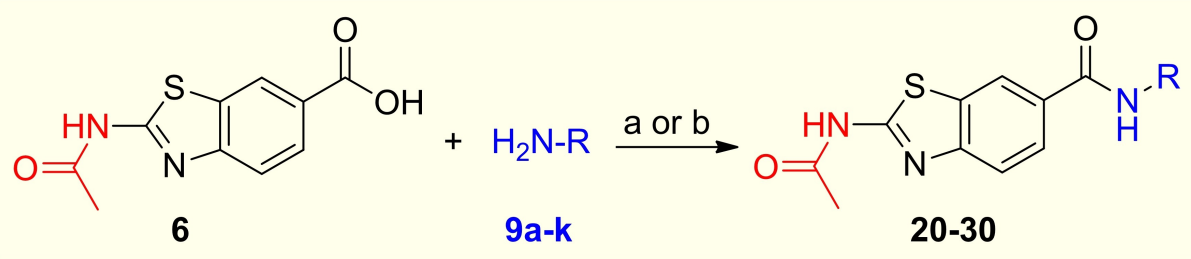

Correspondence amine/final product: **9a/20**; **9b/21**; **9c/22**; **9d/23**; **9e/24**; **9f/25**; **9g/26**; **9h/27**; **9i/28**; **9j/29**; **9k/30**

Scheme 5. General synthetic route for the preparation of the new substituted benzothiazole derivatives **20**–**30**. *Reagents and conditions:* (a) EEDQ/DMF, 80 °C, 3 h and then at r.t. overnight for analogs **20**, **21**, **24**, **27**; (b) EDC, DMAP/DMF, 0 °C, 1 h and then at r.t. the weekend for analogs **22**, **23**, **26**, **28**, **29**, **30**; HOBt instead of DMAP for **25**.

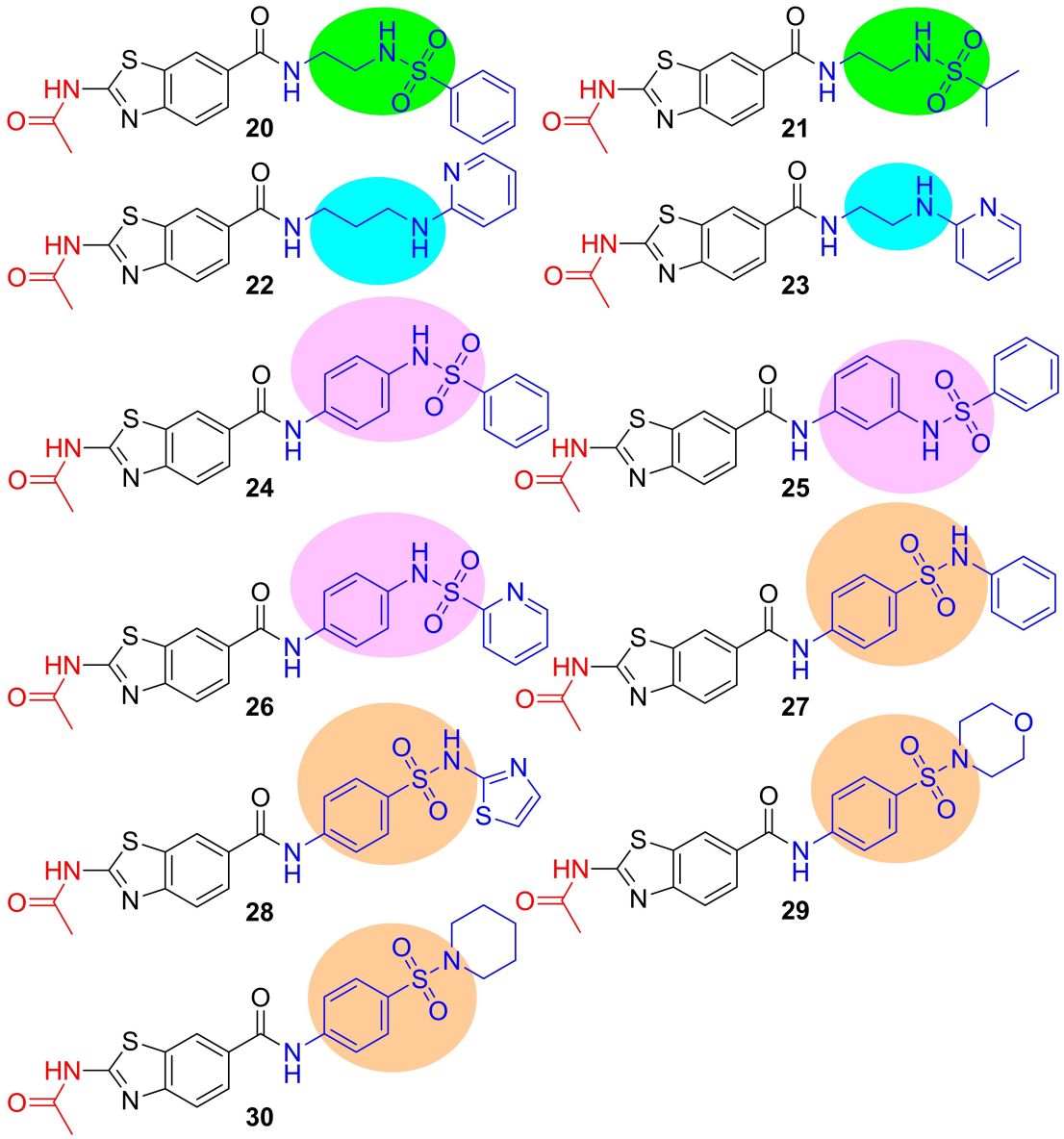

Figure 4. Chemical structures of the new 2-acetamido, 6-carboxamide substituted benzothiazole derivatives.

Biological evaluation of the effects of benzothiazole derivatives on cancer cell-lines

Assessment of cell viability in colorectal cancer (CRC) cell lines. Biological effect on inhibition of ERK1/2 activity

The evaluation of the new benzothiazole derivatives (BTD) was performed in the colon cancer cell lines RKO, HT29 and Colo-205 that bear a heterozygous BRAFV600E mutation. The cytotoxic/cytostatic effect and the MAPK inhibition potential was examined. In order to estimate the potential effect of the newly synthesized benzothiazole derivatives on BRAF pathway activity, we performed western blot analysis to estimate the levels of p-ERK1/2, an established biomarker for BRAF-MEK-ERK pathway activity. A negative control (DMSO 0,1% v/v) and a positive control (**PLX4720**, 1 μM) were evaluated in each case. BRAFV600E mutant cells treated with BTD (1, 5, 10, 20 μM) exhibited reduced viability compared to cell treatment with **PLX4720** under the same conditions.

Treatments with benzothiazole derivative **27** significantly reduced cell viability of RKO and Colo-205 colon adenocarcinoma cells 72 h post-treatment. (Figure 5). For instance, treatment with **27** at a concentration of 10 μM in the culture medium reduced cell viability to 74% και 67%, respectively. On the other hand, treatment with **27** had no effect on the viability of HT29 adenocarcinoma more resistant cells.

BTD compounds **20**, **21** and **23** induced a marginal reduction in colorectal cancer (CRC) cells viability under selected conditions (Figure S44 in SI) after 72 h treatment, with no significant effect on p-ERK1/2 activity (data not shown). Compound **28** also induced marginal effects in CRC cell viability (data not shown).

BTD compounds **24** and **29** did not exhibit any significant effect on CRC cell viability after 72 h treatment, whereas **25** and **30** reduced the viability only at the highest concentration of 20 μM (Figure 6). The effect of 10 μM treatments was not determined for these compounds. Treatment with **25** (20 μM) resulted in 40% (RKO, HT29) or 60% (Colo-205) reduction of cell viability. Treatment with **30** (20 μM) resulted in 30%, 40% and 60% reduction of cell viability for RKO, HT29 and Colo-205, respectively. It should be noted that the *in vitro* inhibition of BRAFV600E activity by these compounds was limited as shown in Table 1.

Furthermore, compound **26** treatments did not affect RKO and Colo-205 and exhibited moderate effect on HT29 cell viability (Figure 7A). However, conditional effects of **26** both at the level of p-ERK1/2 activity and on cell morphology were observed, that are considered of potential interest. In particular, p-ERK1/2 activity was significantly reduced after 24 h treatment of RKO cells with 1–10 μM of **26** (Figure 7B). In addition, treatment of HT-29 and Colo-205 cells with 1–10 μM of **26** for 48 h, resulted in evident effects on cell morphology, as shown in the images taken through the optical microscope (Figures 7C & D).

A particular focus was given to the biological evaluation of compound **22**, which exhibited significant inhibition of the BRAFV600E kinase activity *in vitro* (IC_{50} = 7.9 μM, Table 1). Surprisingly, it showed only marginal effects on CRC cell viability (Figure 8A). Nevertheless, compound **22** treatment (1–20 μM) of Colo-205 cells for 1 or 24 h, induced significant inhibition on p-ERK activity (up to 90% inhibition) (Figure 8B).

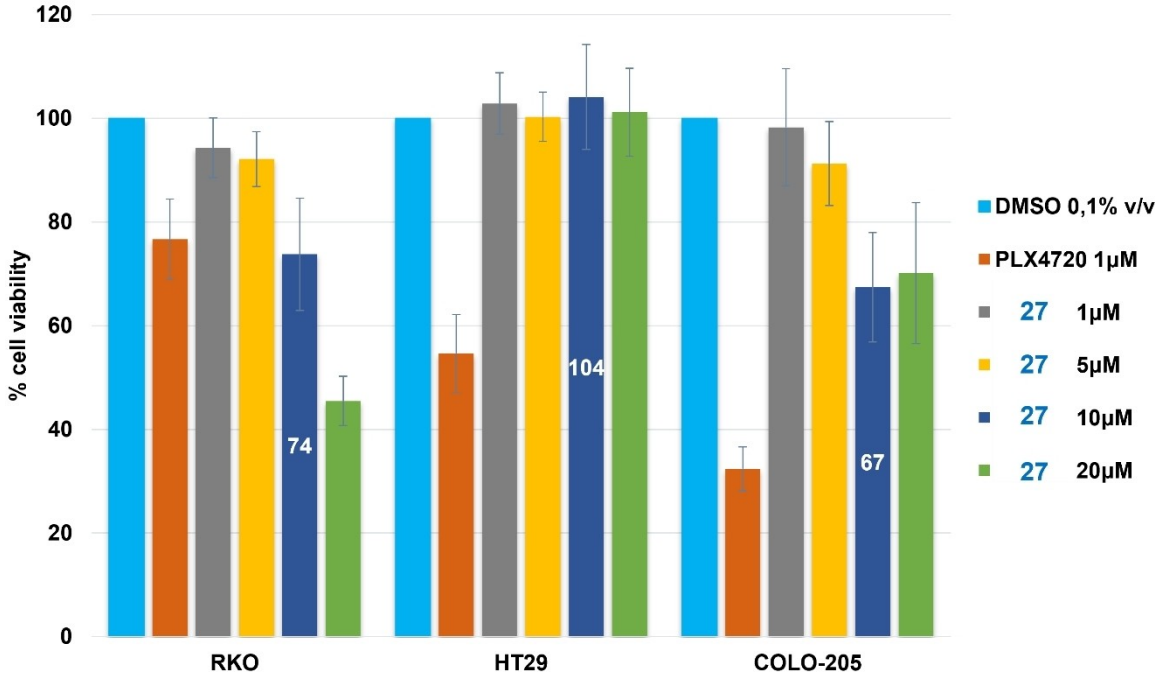

Figure 5. Viability of colon cancer cell lines after 72 h exposure to different concentrations of compound **27**. The effect of 1 μM of **PLX4720**, is also shown. The numbers within the blue bars indicate the % viability for the 10 μM treatment; error bars: ± SD.

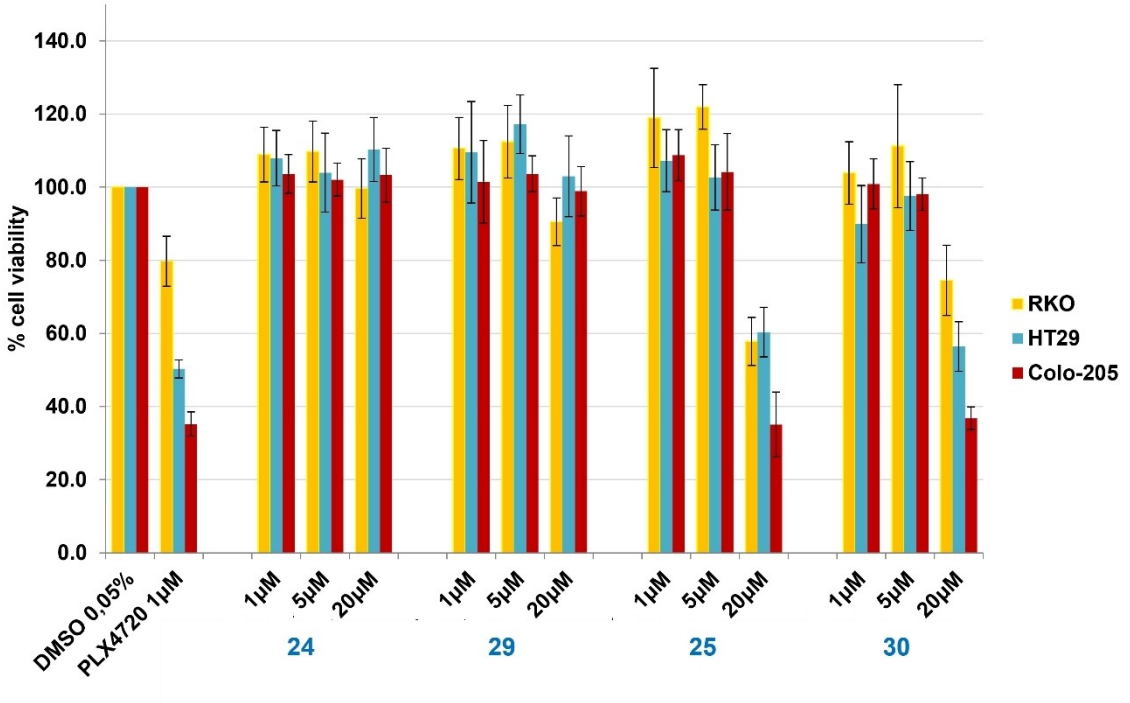

Figure 6. Viability of colon cancer cell lines after 72 h exposure to different concentrations of compounds **24**, **25**, **29**, **30**. The effect of 1 μM of **PLX4720**, is also shown; error bars: ± SD.

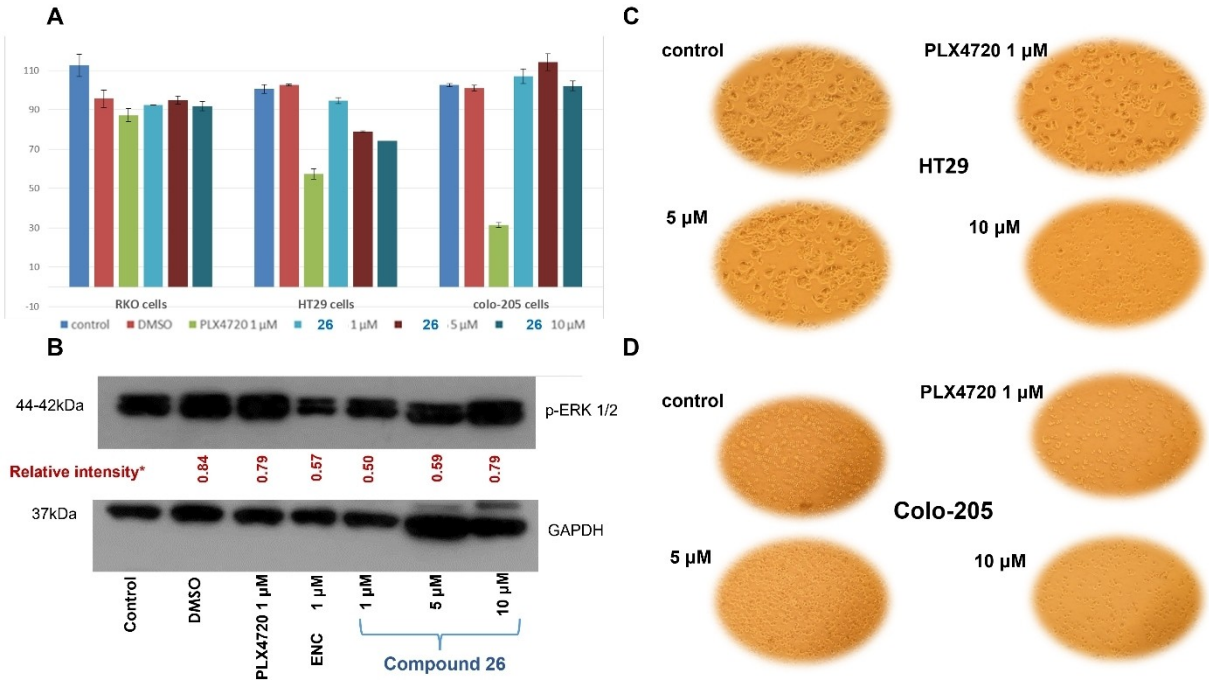

Figure 7. Treatments of CRC cells with compound **26**: (A) cell viability; (B) effects at the level of p-ERK1/2 activity; *the relative intensity values represent the relative to the control normalized p-ERK1/2 to the respective GAPDH band intensities; (C) and (D) effects on cell morphology.

Assessment of cell viability in melanoma cells

The new benzothiazole derivatives (BTD) were also evaluated in melanoma cell lines. One cell line bearing BRAFwt (SK-MEL-2), two cell lines homozygotes for BRAFV600E (A375 and SK-MEL-28), and a cell line heterozygote for the BRAFV600E (MW-164) were chosen to examine the cytotoxic/cytostatic effect of BTD. In the melanoma cell lines, a broader range of concentrations of the compounds under consideration than the range used in colorectal cell lines was used (1, 10, 100 μM) in order to

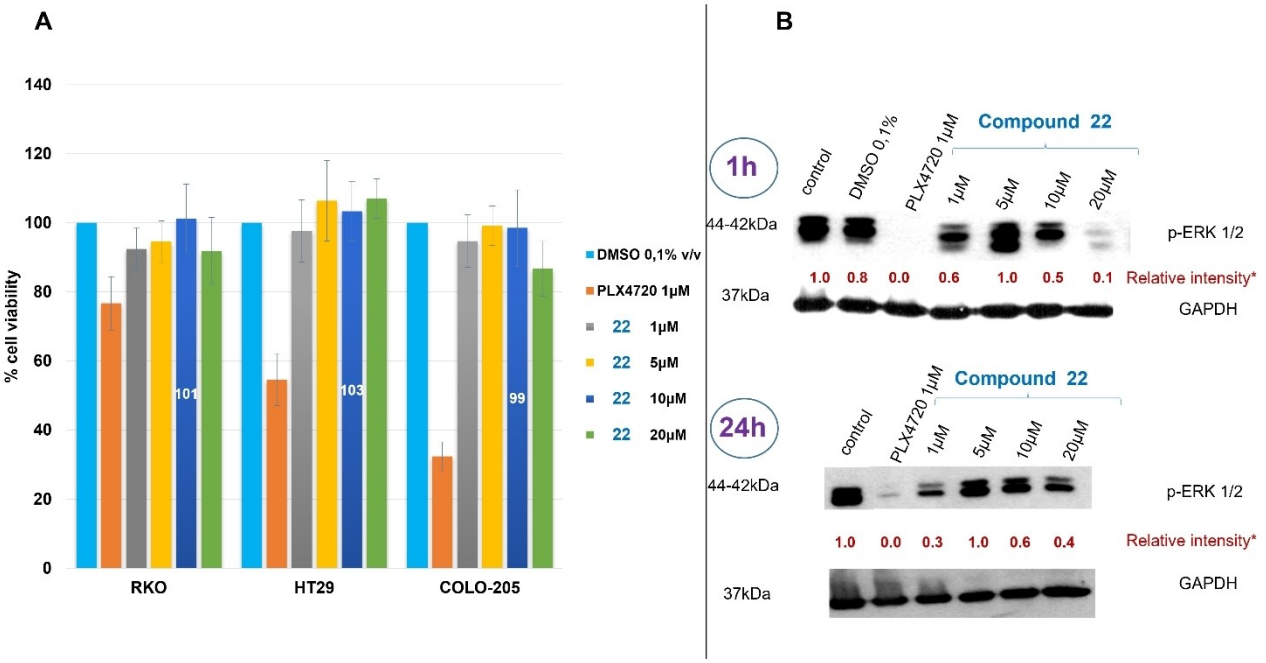

Figure 8. Treatments of CRC cells with compound **22**; (A) cell viability; the numbers within the blue bars indicate the % viability for the 10 μM treatment; error bars: ± SD. (B) effects at the level of p-ERK1/2 activity; *the relative intensity values represent the relative to the control normalized p-ERK1/2 to the respective GAPDH band intensities.

differentiate the cell viability effect more efficiently. The drug Vemurafenib (**PLX4032**, analog of its precursor **PLX4720** lead compound), and the paradox breaker **PLX8394** were used as positive controls to assess melanoma cell viability. Figure 9 shows the effect of **PLX4032** and **PLX8394**, and the benzothiazole derivative **22** on the melanoma cell lines' viability after 72 h of exposure.

The remarkably high viability of SK-MEL-2 observed after exposure to **PLX8394** and **PLX4032**, indicates its resistance of the particular cell line to I1/2 inhibitors, as expected due to its wild-type BRAF genotype (Figure 9). Accordingly, SK-MEL-2 was also resistant to **22** throughout the range of concentrations used. Furthermore, SK-MEL-2 is mutated in the NRAS gene (Q61R mutation), which may lead to BRAF dimerization,

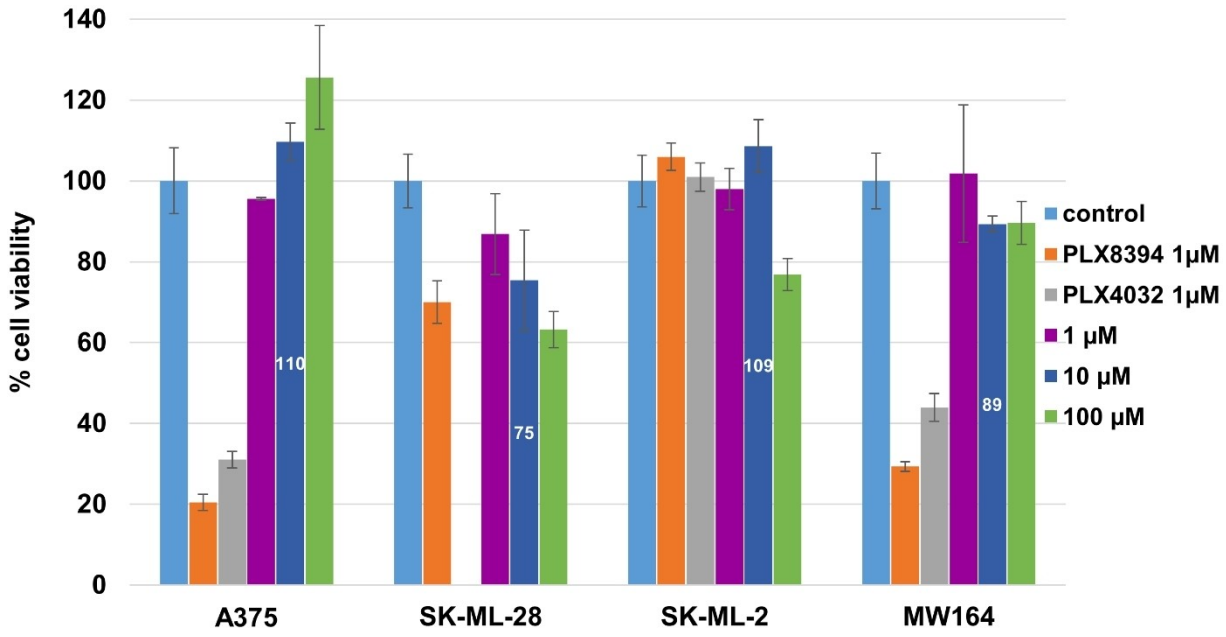

Figure 9. Viability of melanoma cell lines after 72 h exposure to different concentrations of compound **22**. The effect of 1 μM of the paradox breaker **PLX8394** and **PLX4032** are also shown. The numbers within the blue bars indicate the % viability for the 10 μM treatment; error bars: ± SD; ND: not determined.

continuous pathway activation, and cell proliferation. A375, SK-MEL-28, and MW164 were shown to be sensitive in PLX inhibitors in the order A375 > MW164 > SK-ML28. As mentioned above, A375 and SK-MEL-28 are both homozygotes for BRAFV600E. However, the lower sensitivity of SK-MEL-28 in PLX compounds relative to that observed for A375 could be attributed to its homozygosity for the 2257 C > T EGFR (Pro753Ser) mutation, which is found in squamous cell carcinomas and classified as possibly pathogenic.[37] Treatments with compound **22** for 72 h resulted in a marginal, but however, statistically significant reduction of cell viability of SK-MEL28 and MW164 even at low concentrations but not of A375. After exposure to 10 μM of **22** the viability was reduced to 75% ($t(8) = -4.052$, $p < 0.001$) and 89% ($t(8) = -3.440$, $p = 0.009$) for SK-ML-28 and MW-164, respectively. It is noteworthy to mention the reduction of SK-ML-28 viability to 87% even at the lowest concentration of 1 μM of **22** ($t(8) = -2.416$, $p = 0.042$).

The effects of the benzothiazole derivatives **20**, **27**, and **28** on the melanoma cell lines' viability were qualitatively similar but less pronounced than the effects of **22**. All compounds throughout the range of concentrations used did not affect A375 and SK-MEL-2 cells (Figure S45 in SI). All compounds caused a modest but consistent decrease in MW164 viability, whereas **20** and **27** also caused a marginal reduction in SK-MEL-28 cell viability.

As mentioned above, A375 and MW-164 cell lines were more sensitive to the BRAFV600E selective inhibitors, **PLX8394**, and **PLX4032** than the other melanoma cell lines. Therefore, it was decided to test three additional BTD derivatives, **24**, **25** and **29**, in one of them, the MW-164 cell line. In order to obtain comprehensive viability curves, ten concentrations were used (0.00, 1.56, 3.13, 6.25, 10.00, 12.50, 20.00, 25.00, 50.00, 100.00 μM), and the results are shown in Figure 10.

Compounds **24** and **29** did not have any effect on WM-164 cell survival. However, compound **25** caused a significant reduction of cell viability, particularly in the higher concentrations, and probit analysis gave a concentration for 50% inhibition of cell proliferation (IC_{50}) of 37.2 μM. The results presented in Figure 10 directly reflect the results of Figure 6 observed for the colorectal cancer cell lines.

Effect of compound 22 on gene expression and major pathway regulation as shown by next-generation sequencing

A global gene expression profile was performed to elucidate the involved pathways and genes, based on the inhibitory effects of compound **22** on p-ERK1/2 activity in Colo-205 cells and cell proliferation of various CRC and melanoma cell lines tested.

Gene expression profiling of Colo-205 cells upon 24 h treatment with two different concentrations of compound **22** revealed mild changes at the level of gene expression. In particular, 88 differentially expressed genes as compared to DMSO-treated cells (57 upregulated, 31 downregulated) were identified after treatment with 1 μM of compound **22** and 161 differentially expressed genes (74 upregulated, 87 downregulated) were identified after treatment with 10 μM of compound **22** (Tables S2 & S3 in SI).

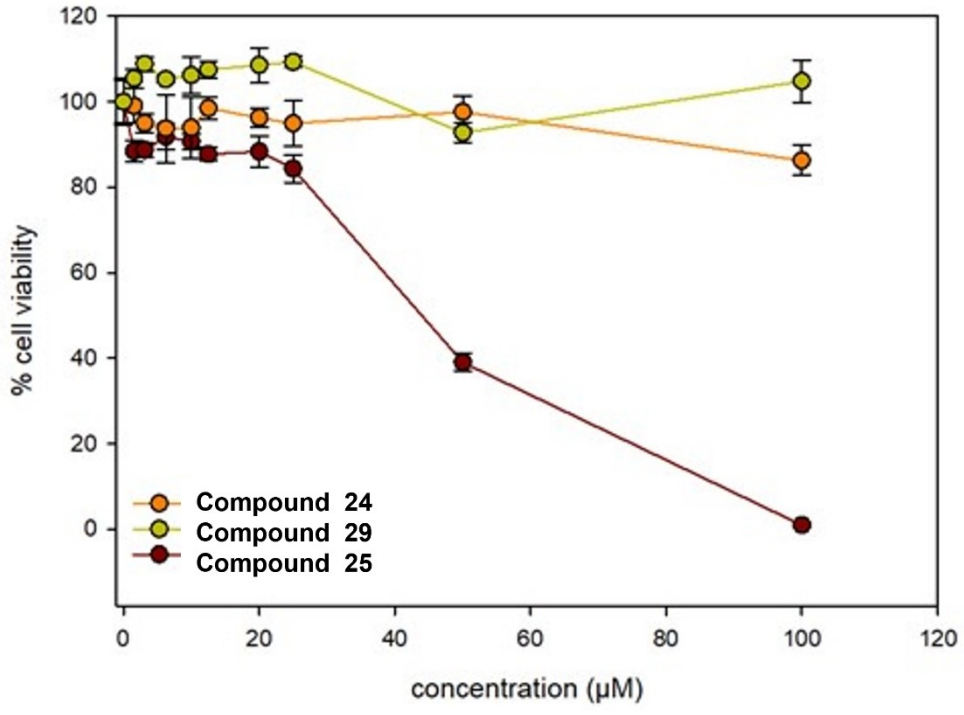

Figure 10. Viability curves of the cancer cell line WM-164 treated with derivatives **24**, **25**, **29** for 72 h in concentrations ranging from 0 to 100 μM using the MTT assay; error bars: ± SD.

Based on Gene Ontology (GO) Biological Process enrichment, functional analysis for each set of differentially expressed genes was performed on BioInfoMiner platform, revealing common alterations like xenobiotic metabolism and response to hypoxia. Statistically significant enriched GO terms are grouped according to their biological relevance and presented in Figure 11. Interestingly, treatment with 1 μM of compound **22** seems to affect apoptotic signalling, since several apoptosis-related genes are overexpressed. In particular, the pro-apoptotic genes[38] of the BCL2 family –Bcl2 modifying factor (*BMF*) and BCL2 interacting protein 3 (*BNIP3*) were upregulated by compound **22**, as well as the member of the TNF ligand family TNF Superfamily Member 12 (*TNFSF12*).[39]

Conclusions

In the context of this work, eleven new substituted benzothiazole derivatives were designed and synthesized in an effort to provide efficient inhibitors of the BRAFV600E oncogenic kinase and tackle drug resistance often developed during cancer treatment. Synthesis was achieved by coupling of 2-acetamidobenzo[d]thiazole-6-carboxylic acid with the appropriate amines possessing an alkylene or phenylene linker between the primary amino group (NH_2) and the terminal functionality. Among these analogs, 2-acetamido-*N*-[3-(pyridin-2-ylamino)propyl]benzo[d]thiazole-6-carboxamide (**22**), exhibited significant inhibition of the BRAFV600E kinase activity *in vitro* (IC_{50} = 7.9 μM), and although it displayed lower inhibition against BRAFV600E as compared to the drug Vemurafenib, a notable selectivity against wtBRAF was observed. Hence, particular focus was given to its further biological evaluation in colorectal cancer and melanoma cell lines. Although it showed only marginal effects on colorectal cancer cells' viability, **22** treatment (1–20 μM) of Colo-205 cells for 1 or 24 h, induced significant inhibition (up to 90%) of p-ERK activity. Gene expression profiling of Colo-205 cells upon 24 h treatment with two different concentrations of **22** (1 and 10 μM) revealed mild changes at the level of gene expression. Interestingly, treatment with 1 μM **22** affected apoptotic signaling, since several apoptosis-related genes, such as the pro-apoptotic genes of the BCL2 family-Bcl2 modifying factor (BMF) and BCL2 interacting protein 3 (BNIP3), were found overexpressed. On the other hand, treatment of various melanoma cell lines with **22** at 1, 10, 100 μM resulted in a statistically significant reduction of cell viability in SK-MEL-28 and MW164 cells only. Overall, **22** was the only analog among the newly synthesized benzothiazole derivatives providing promising results in all assays applied, which paves the way for further investigation in view of its use in drug development.

Experimental Section

In silico studies

All benzothiazole derivatives were primarily sketched and then were prepared at the optimum pH = 7.0 ± 0.5, using LigPrep program[40] of MAESTRO.[41] Subsequently, the crystal structure of BRAFV600E complexed with **PLX7904** (PDB: 4XV1, Resolution: 2.47 Å) was subjected to Protein Preparation[42] and a grid box with the following dimensions was generated, 10×10×10 Å. Molecular docking simulations were performed to all examined compounds, applying the Extra- Precision (XP) mode of Glide,[43] identifying their favorable binding configurations. The validation process indicated that the RMSD value, between the co-crystallized and docked **PLX7904**, was equal to 0.3916 Å. The docking poses were visually inspected and their binding modes were analyzed. The physicochemical profile of the examined benzothiazoles was also predicted.[44]

Chemistry

General

The experimental part for the preparation of compounds **2**–**6**, **9a**–**k**, **13**, **15** and **19a**–**d** is presented in detail in SI. All other chemicals were commercially available. Experiments with US irradiation were performed in a FALK ultrasound bath apparatus. NMR spectra were recorded on a Varian 300 (300.13 MHz and 75.47 MHz for ^1H and ^{13}C

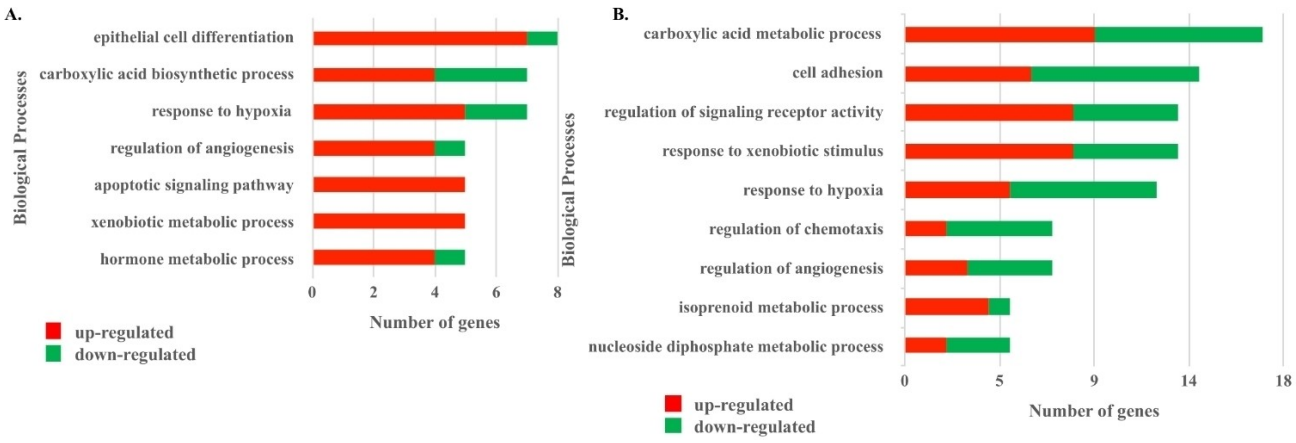

Figure 11. Statistically significant biological processes with the corresponding number of genes after treatment of Colo-205 colorectal cancer cells with 1 μM (A) or 10 μM (B) of compound **22**. Only processes containing a minimum number of five genes are shown. The number of significantly differentiated genes involved in each process is shown on the x axis, red and green colour correspond to up- or down-regulation, respectively.

{^{1}H}, respectively) or a Varian 600 (599.827 MHz and 150.842 MHz for ^{1}H and ^{13}C{^{1}H}, respectively). The assignment of protons and carbons in the ^{1}H and ^{13}C NMR spectra was performed by HSQC NMR spectra. Chemical shift values in ^{1}H and ^{13}C NMR spectra were referenced internally to the residual solvent resonances. High resolution mass spectrometry (HRMS) was determined by a Thermo Scientific LTQ Orbitrap Velos (ESI); experimental details for the positive and negative ESI-MS or APCI of the final compounds in DMSO/MeOH (10:90): source voltage (KV): 3 (**22**, **23**, **24**, **26**, **28**), 4 (**20**, **21**, **27**), 5 (**25**, **29**, **30**); source temperature (°C): 100 (**27**), 200 (**20**, **21**, **25**, **29**, **30**); vaporizer temperature (°C): 300 (**22**, **23**, **28**), 350 (**24**, **26**); sheath gas flow rate (arb): 15 (**27**), 18 (**25**, **29**, **30**), 20 (**20**, **21**), 30 (**24**, **26**, **28**), 50 (**22**, **23**); aux gas flow rate (arb): 5 (**20**, **21**, **22**, **23**, **25**, **27**, **29**, **30**), 10 (**24**, **26**, **28**); sweep gas flow rate (arb): 5 (**22**, **23**); capillary temperature (°C): 270 (**27**), 275 (**20**, **21**, **22**, **23**, **25**, **29**, **30**), 350 (**24**, **26**, **28**). Melting points were measured on a Büchi melting point apparatus. The purity of the target molecules was determined by high-performance liquid chromatography (HPLC) (Thermo Scientific HPLC SPECTRASYSTEM with a Thermo Scientific SPECTRASYSTEM UV2000 detector and a EC 250/4.6 NUCLEOSIL 100–5 C18 HD column, using the following analytical method: gradient elution 20/80 CH_3CN/H_2O to 100/0 over 20 min; UV detection at 285, 286, 294, 299, 301, 302 and 306 nm; flow rate 1 mL/min; injection volume 20 μL. The purity of all final products was over 96%.

2-Acetamido-N-[2-(phenylsulfonamido)ethyl]benzo[d]thia-zole-6-carboxamide (20)

To a stirring solution of 2-acetamidobenzo[d]thiazole-6-carboxylic acid (**6**) (100 mg, 0.42 mmol) and EEDQ (0.55 mmol) in DMF (1.5 mL) at a pressure of ~25 mm Hg, a solution of *N*-(2-aminoethyl)benzenesulfonamide (**9a**) (100 mg, 0.42 mmol) in DMF (1.5 mL) was added. The resulting mixture was left stirring for 3 h at 80 °C and then at room temperature overnight at ambient pressure. The DMF was then removed under reduced pressure, water was added (80 mL) and the mixture was extracted with ethyl acetate (3×100 mL). The combined organic layers were washed with brine (1×200 mL), dried over sodium sulfate and concentrated under reduced pressure to afford the crude product, which was purified by flash chromatography (ethyl acetate/CH_2Cl_2, 8:2) to give **20** (R_f = 0.37) as a white solid (45 mg, 26%), m.p. >200 °C. ^{1}H NMR (600 MHz, DMSO-d_6): δ 12.46 (bs, 1H), 8.51 (t, J = 5.6 Hz, 1H), 8.39 (d, J = 1.4 Hz, 1H), 7.86 (dd, J = 8.5, 1.7 Hz, 1H), 7.81–7.79 (m, 2H), 7.76–7.75 (d, J = 8.5 Hz, 1H), 7.62–7.56 (m, 3H), 3.34–3.31 (m, 2H), 2.93 (m, 2H), 2.21 (s, 3H). ^{13}C NMR (75.47 MHz, DMSO-d_6): δ 169.80, 166.12, 160.06, 150.66, 140.42, 132.49, 131.32, 129.55, 129.31, 126.50, 125.45, 121.22, 119.95, 42.01, 39.40, 22.87. HRMS (ESI): calculated for $C_{18}H_{17}N_4O_4S_2$ $[M-H]^-$ 417.0689; found 417.0689. HPLC analysis: t_R = 6.81 min, detection at 286 nm, purity = 98.9%.

2-Acetamido-N-[2-(1-methylethylsulfonamido)ethyl]benzo[d] thiazole-6-carboxamide (21)

It was synthesized as described for **20** from **6** (89 mg, 0.34 mmol), EEDQ (0.55 mmol) in DMF (1.5 mL) and *N*-(2-aminoethyl)propane-2-sulfonamide (**9b**) (70 mg, 0.42 mmol) in DMF (1.5 mL). The crude product was purified by flash chromatography (CH_2Cl_2/methanol, 9:1) to give **21** (R_f = 0.25; ethyl acetate/CH_2Cl_2, 8:2) as a light yellow solid (45 mg, 35%), m.p. >200 °C.^{1}H NMR (600 MHz, DMSO-d_6): δ 12.48 (br s, 1H), 8.54 (t, J = 5.5 Hz, 1H), 8.44 (d, J = 1.3 Hz, 1H), 7.91 (dd, J = 8.5, 1.6 Hz, 1H), 7.77 (d, J = 8.5 Hz, 1H), 7.17 (t, J = 6.0 Hz, 1H), 3.39–3.36 (m, 2H), 3.20–3.12 (m, 3H), 2.22 (s, 3H), 1.22 (d, J = 6.8 Hz, 6H). ^{13}C NMR (75.47 MHz, DMSO-d_6): δ 169.75, 166.06, 160.07, 150.62, 131.30, 129.59, 125.35, 121.17, 119.88, 51.47, 41.99, 40.20, 22.85, 16.34. HRMS (ESI): calculated for $C_{15}H_{19}N_4O_4S_2$ $[M-H]^-$ 383.0846; found 383.0845. HPLC analysis: t_R = 5.98 min, detection at 286 nm, purity = 100%.

2-Acetamido-N-[3-(pyridin-2-ylamino)propyl]benzo[d]thia-zole-6-carboxamide (22)

To a mixture of N^1-(pyridin-2-yl)propane-1,3-diamine (**9c**) (128 mg, 0.84 mmol), **6** (200 mg, 0.84 mmol) and DMAP (20 mg, 0.17 mmol) in DMF (9 mL), EDC (243 mg, 1.05 mmol) was added at 0 °C. The reaction mixture was left stirring for an hour at 0 °C and then at room temperature over the weekend. The DMF was then removed under reduced pressure and the mixture was extracted with ethyl acetate (2×50 mL) and the combined organic layers were washed with water (1×100 mL), dried over sodium sulfate and concentrated under reduced pressure to afford the crude product which was purified by flash chromatography (CH_2Cl_2/MeOH, 90:10 to 85:15) to afford **22** (R_f = 0.4; CH_2Cl_2/MeOH, 85:15) as a white solid (150 mg, 48%), m.p. >200 °C. ^{1}H NMR (600 MHz, DMSO-d_6): δ 12.46 (br s, 1H), 8.54 (t, J = 5.5 Hz, 1H), 8.43 (m, 1H), 7.94 (d, J = 3.9 Hz, 1H), 7.90 (dd, J = 8.5, 1.5 Hz, 1H), 7.76 (d, J = 8.4 Hz, 1H), 7.35–7.33 (m, 1H), 6.49–6.43 (m, 3H), 3.31–3.27 (m, 4H), 2.21 (s, 3H), 1.80–1.77 (m, 2H). ^{13}C NMR (75.47 MHz, DMSO-d_6): δ 169.80, 165.91, 160.06, 158.90, 150.55, 147.53, 136.58, 131.35, 129.91, 125.34, 121.07, 119.91, 111.36, 108.10, 38.48, 37.36, 29.17, 22.88. HRMS (APCI): calculated for $C_{18}H_{20}N_5O_2S$ $[M+H]^+$ 370.1332; found 370.1331. HPLC analysis: t_R = 6.88 min, detection at 285 nm, purity = 97.6%.

2-Acetamido-N-[2-(pyridin-2-ylamino)ethyl]benzo[d]thiazole-6-carboxamide (23)

It was synthesized as described for **22** from N^1-(pyridin-2-yl)ethane-1,2-diamine (**9d**) (60 mg, 0.44 mmol), **6** (100 mg, 0.44 mmol), DMAP (10 mg, 0.09 mmol) in DMF (4.5 mL) and EDC (105 mg, 0.55 mmol). The crude product was purified by flash chromatography (CH_2Cl_2/MeOH, 9:1) to afford **23** (R_f = 0.7; CH_2Cl_2/MeOH, 9:1) as a white solid (50 mg, 32%), m.p. >200 °C. ^{1}H NMR (600 MHz, DMSO-d_6): δ 12.48 (br s, 1H), 8.65 (t, 1H), 8.44 (m, 1H), 7.98–7.97 (m, 1H), 7.91 (dd, J = 8.5, 1.7 Hz, 1H), 7.77 (d, J = 8.4 Hz, 1H), 7.37 (td, J = 7.9, 7.1, 1.9 Hz, 1H), 6.62 (t, 1H), 6.49–6.47 (m, 2H), 3.44 (m, 4H), 2.22 (s, 3H). ^{13}C NMR (75.47 MHz, DMSO-d_6): δ 169.73, 166.04, 160.01, 158.79, 150.55, 147.47, 136.69, 131.30, 129.77, 125.33, 121.10, 119.87, 111.62, 108.14, 40.07, 39.80, 22.84. HRMS (APCI): calculated for $C_{17}H_{18}N_5O_2S$ $[M+H]^+$ 356.1176, found 356.1177. HPLC analysis: t_R = 6.51 min, detection at 294 nm, purity = 98.5%.

2-Acetamido-N-[4-(phenylsulfonamido)phenyl]benzo[d]thia-zole-6-carboxamide (24)

It was synthesized as described for **20** from **6** (100 mg, 0.42 mmol), EEDQ (247 mg, 0.53 mmol) in DMF (1.5 mL) and *N*-(4-aminophenyl)benzenesulfonamide (**9e**) (132 mg, 0.53 mmol) in DMF (1.5 mL). The crude product was washed with ethyl acetate and methanol to afford **24** (R_f = 0.41; ethyl acetate/CH_2Cl_2, 8:2) as a white solid (68 mg, 35%), m.p. >200 °C. ^{1}H NMR (600 MHz, DMSO-d_6): δ 12.51 (br s, 1H), 10.23 (s, 1H), 10.15 (br s, 1H), 8.53–8.52 (m, 1H), 7.97 (dd, J = 8.5, 1.5 Hz, 1H), 7.81 (d, J = 8.5 Hz, 1H), 7.74 (d, J = 7.4 Hz, 2H), 7.63–7.60 (m, 3H), 7.56–7.53 (m, 2H), 7.06 (d, J = 8.8 Hz, 2H), 2.22 (s, 3H). ^{13}C NMR (75.47 MHz, DMSO-d_6): δ 169.74, 164.94, 160.29, 150.86, 139.46, 135.91, 133.00, 132.82, 131.33, 129.94, 129.21, 126.68, 125.83, 121.64, 121.29, 121.06, 120.00, 22.83. HRMS (APCI): calculated for $C_{22}H_{19}N_4O_4S_2$ $[M+H]^+$ 467.0842; found 467.0849. HPLC analysis: t_R = 7.75 min, detection at 299 nm, purity = 100%.

2-Acetamido-N-[3-(phenylsulfonamido)phenyl]benzo[d]thiazole-6-carboxamide (25)

It was synthesized as described for **22** from *N*-(4-aminophenyl)benzenesulfonamide (**9f**) (100 mg, 0.4 mmol), **6** (95 mg, 0.4 mmol), HOBt (85 mg, 0.63 mmol) instead of DMAP in DMF (7 mL) and EDC (100 mg, 0.5 mmol). The crude product was purified by flash chromatography (ethyl acetate/CH_2Cl_2, 8:2) to afford **25** (R_f = 0.63) as a white solid (40 mg, 22%), m.p. > 200 °C. ^{1}H NMR (600 MHz, DMSO-d_6): δ 12.52 (brs, 1H), 10.30 (s, 2H), 8.55 (s, 1H), 7.99 (d, J = 8.2 Hz, 1H), 7.81 (m, 3H), 7.73 (s, 1H), 7.57–7.54 (m, 3H), 7.45 (d, J = 7.6 Hz, 1H), 7.17 (t, J = 8.0 Hz, 1H), 6.81 (d, J = 7.6 Hz, 1H), 2.23 (s, 3H). ^{13}C NMR (75.47 MHz, DMSO-d_6: δ 171.42, 166.70, 161.43, 151.63, 140.38, 139.86, 138.65, 134.12, 132.19, 130.59, 130.38, 130.23, 127.62, 126.93, 122.52, 121.11, 117.30, 116.33, 112.92, 23.59. HRMS (ESI): calculated for $C_{22}H_{19}N_4O_4S_2$ $[M+H]^+$ 467.0842, found 467.0840; calculated for $C_{22}H_{17}N_4O_4S_2$ $[M-H]^-$ 465.0697, found 465.06833; calculated for $C_{22}H_{18}N_4O_4NaS_2$ $[M+Na]^+$ 489.0662, found 489.0656.

2-Acetamido-N-[4-(pyridine-2-sulfonamido)phenyl]benzo[d]thiazole-6-carboxamide (26)

It was synthesized as described for **22** from *N*-(4-aminophenyl)pyridine-2-sulfonamide (**9g**) (40 mg, 0.16 mmol), **6** (38 mg, 0.16 mmol), DMAP (4 mg, 0.03 mmol) in DMF (1.5 mL) and EDC (38 mg, 0.2 mmol). The crude product was purified by flash chromatography (ethyl acetate/CH_2Cl_2, 8:2) to afford **26** (R_f = 0.37) as a white solid (40 mg, 53%), m.p. > 200 °C. ^{1}H NMR (600 MHz, DMSO-d_6): δ 12.51 (br s, 1H), 10.43 (br s, 1H), 10.21 (s, 1H), 8.73–8.72 (m, 1H), 8.53–8.52 (m, 1H), 8.05–8.02 (m, 1H), 7.97–7.95 (m, 1H), 7.93–7.92 (m, 1H), 7.80 (dd, J = 8.5, 2.4 Hz, 1H), 7.65–7.59 (m, 3H), 7.11–7.09 (m, 2H), 2.22 (s, 3H). ^{13}C NMR (150.84 MHz, DMSO-d_6): δ 169.71, 167.27, 164.89, 160.27, 156.51, 150.84, 150.09, 138.64, 135.66, 131.31, 129.92, 127.26, 125.80, 122.48, 121.61, 121.28, 120.98, 119.97, 22.81. HRMS (APCI): calculated for $C_{21}H_{18}N_5O_4S_2$ $[M+H]^+$ 468.0800, found 468.0788; calculated for $C_{21}H_{16}N_5O_4S_2$ $[M-H]^-$ 466.0644, found 466.0636. HPLC analysis: t_R = 7.03 min, detection at 301 nm, purity = 96.5%.

2-Acetamido-N-[4-(N-phenylsulfamoyl)phenyl]benzo[d]thiazole-6-carboxamide (27)

It was synthesized as described for **20** from **6** (76 mg, 0.32 mmol), EEDQ (99 mg, 0.40 mmol) in DMF (1 mL) and 4-amino-*N*-phenylbenzenesulfonamide (**9h**) (100 mg, 0.40 mmol) in DMF (1 mL). The crude product was purified by flash chromatography (ethyl acetate/CH_2Cl_2, 8:2) to give **27** (R_f = 0.58) as a white solid (30 mg, 20%), m.p. > 200 °C. ^{1}H NMR (600 MHz, DMSO-d_6,): δ 10.61 (s, 1H), 8.56 (s, 1H), 8.00–7.98 (m, 1H), 7.93 (d, J = 8.7 Hz, 2H), 7.83 (d, J = 8.5 Hz, 1H), 7.74 (d, J = 8.7 Hz, 2H), 7.22 (t, J = 7.8 Hz, 2H), 7.09 (d, J = 7.8 Hz, 2H), 7.01 (t, J = 7.2 Hz, 1H), 2.22 (s, 3H). ^{13}C NMR (150.84 MHz, DMSO-d_6): δ 169.87, 165.68, 160.65, 151.22, 143.19, 137.95, 133.66, 131.42, 129.43, 129.14, 127.80, 126.04, 123.92, 121.99, 120.09, 120.03, 119.83, 22.88. HRMS (ESI): calculated for $C_{22}H_{19}N_4O_4S_2$ $[M+H]^+$ 467.0842, found 467.0835; calculated for $C_{22}H_{18}N_4O_4NaS_2$ $[M+Na]^+$ 489.06662, found 489.0652; calculated for $C_{22}H_{17}N_4O_4S_2$ $[M-H]^-$ 465.0697, found 465.0694. HPLC analysis: t_R = 8.19 min, detection at 302 nm, purity = 97.2%.

2-Acetamido-N-[4-(N-thiazol-2-ylsulfamoyl)phenyl]benzo[d]thiazole-6-carboxamide (28)

It was synthesized as described for **22** from 4-amino-*N*-(thiazol-2-yl)benzenesulfonamide (**9i**) (160 mg, 0.64 mmol), **6** (150 mg, 0.64 mmol), DMAP (16 mg, 0.13 mmol) in DMF (7 mL) and EDC (190 mg, 0.80 mmol). After the usual workup, the combined organic layers were washed with water (1×100 mL), and a solid was formed in the aqua layer, which was collected by filtration and dried at vacuum pump in order to afford **28** (R_f = 0.47; $CHCl_3$/MeOH, 8:2) as a light orange solid (60 mg, 20%), m.p. (dec. 180–182 °C). ^{1}H NMR (600 MHz, DMSO-d_6): δ 12.70 (br s, 1H), 12.55 (s, 1H), 10.61 (s, 1H), 8.59 (m, 1H), 8.03–8.01 (dd, 1H), 7.95 (d, J = 8.7 Hz, 2H), 7.84 (d, J = 8.5 Hz, 1H), 7.79 (d, J = 8.7 Hz, 2H), 7.25 (d, J = 4.6 Hz, 1H), 6.82 (d, J = 4.6 Hz, 1H), 2.23 (s, 3H). ^{13}C NMR (75.47 MHz, DMSO-d_6): δ 169.82, 168.74, 165.56, 160.54, 151.16, 142.56, 136.66, 131.42, 129.54, 126.82, 126.07, 124.46, 121.99, 120.11, 119.77, 108.16, 22.85. HRMS (APCI): calculated for $C_{19}H_{16}N_5O_4S_3$ $[M+H]^+$ 474.0359; found 474.0370. HPLC analysis: t_R = 5.93 min, detection at 306 nm, purity = 95.5%.

2-Acetamido-N-[4-(morpholinosulfonyl)phenyl]benzo[d]thiazole-6-carboxamide (29)

It was synthesized as described for **22** from 4-(morpholinosulfonyl)aniline (**9j**) (150 mg, 0.62 mmol), **6** (145 mg, 0.62 mmol), DMAP (15 mg, 0.12 mmol) in DMF (6 mL) and EDC (150 mg, 0.77 mmol). The crude product was purified by flash chromatography (ethyl acetate/CH_2Cl_2, 8:2) to afford **29** (R_f = 0.46) as a white solid (55 mg, 20%), m.p. > 200 °C. ^{1}H NMR (600 MHz, DMSO-d_6): δ 12.55 (br s, 1H), 10.72 (s, 1H) 8.62 (m, 1H), 8.09 (d, J = 8.7 Hz, 2H), 8.04–8.03 (m, 1H), 7.86 (d, J = 8.5 Hz, 1H), 7.74 (d, J = 8.7 Hz, 2H), 3.64–3.63 (m, 4H), 2.88–2.87 (m, 4H), 2.24 (s, 3H). ^{13}C NMR (150.84 MHz, DMSO-d_6): δ 169.79, 165.76, 160.60, 151.23, 143.79, 131.43, 129.42, 128.78, 128.37, 126.08, 122.04, 120.12, 119.92, 65.29, 45.94, 22.84. HRMS (ESI): calculated for $C_{20}H_{21}N_4O_5S_2$ $[M+H]^+$ 461.0948, found 461.0947; calculated for $C_{20}H_{20}N_4O_5NaS_2$ $[M+Na]^+$ 483.0767, found 483.0766; calculated for $C_{20}H_{18}N_4O_5S_2$ $[M-H]^-$ 459.0802, found 459.0788. HPLC analysis: t_R = 7.59 min, detection at 302 nm, purity = 97.5%.

2-Acetamido-N-[4-(piperidin-1-ylsulfonyl)phenyl]benzo[d]thiazole-6-carboxamide (30)

It was synthesized as described for **22** from 4-(piperidin-1-ylsulfonyl)aniline (**9k**) (80 mg, 0.34 mmol), **6** (80 mg, 0.34 mmol), DMAP (10 mg, 0.07 mmol) in DMF (3.5 mL) and EDC (80 mg, 0.43 mmol). The crude product was purified by flash chromatography (ethyl acetate/CH_2Cl_2, 8:2)) to afford **30** (R_f = 0.58) as a white solid (32 mg, 20%), m.p. > 200 °C. ^{1}H NMR (600 MHz, DMSO-d_6): δ 10.69 (s, 1H) 8.61 (s, 1H), 8.07–8.02 (m, 3H), 7.85 (d, J = 8.5 Hz, 1H), 7.73 (d, J = 8.7 Hz, 2H), 2.88 (m, 4H), 2.23 (s, 3H), 1.55 (m, 4H), 1.36 (m, 2H). ^{13}C NMR (75.47 MHz, DMSO-d_6): δ 169.86, 165.72, 151.24, 143.44, 140.91, 132.41, 131.43, 129.43, 128.52, 126.05, 122.01, 120.08, 119.86, 109.57, 46.63, 24.69, 22.88. HRMS (ESI): calculated for $C_{21}H_{23}N_4O_4S_2$ $[M+H]^+$ 459.1155, found 459.1150; calculated for $C_{21}H_{21}N_4O_4S_2$ $[M-H]^-$ 457.1010, found 459.0997; calculated for $C_{21}H_{22}N_4O_4NaS_2$ $[M+Na]^+$ 481.0975, found 481.0966. HPLC analysis: t_R = 8.77 min, detection at 302 nm, purity = 99.2%.

Biology

Kinase activity assay

Compounds were screened for their inhibitory activity against BRAFV600E (BRAFV599E) and wtBRAF via Z'-LYTE™ fluorescent kinase assay technology (Invitrogen, USA) provided through SelectScreen Kinase Profiling Services, Thermo Fisher Scientific, WI USA.[45]

Control BRAF Inhibitors

BRAF inhibitor **PLX4720** was used as a positive control for the biological assessment in CRC cell lines whereas, for the assessment of melanoma cell viability, Vemurafenib (**PLX4032**, analog of its precursor **PLX4720** lead compound), the commercially available drug used for the treatment of late-stage melanoma[46] and the paradox breaker **PLX8394** (in clinical trials) were purchased from Selleckchem, Houston, TX, USA and were used as positive controls. Before the experiment, the inhibitors were diluted in the appropriate for each cell line culture medium.

Cell lines and cultures

Colorectal cancer cell lines

Colo-205, HT29 and RKO human colorectal adenocarcinoma cell lines bearing BRAFV600E were obtained from the American Type Culture Collection (ATCC). Presence of BRAF mutations and/or main non-BRAF driver mutations (in agreement to https://cancer.sanger.ac.uk/cell_lines) have been previously confirmed. All cell lines were grown in DMEM medium supplemented with 10% Fetal Bovine Serum and 1% penicillin/streptomycin and amino acids (all from Thermo Fisher Scientific, Waltham, MA, USA) at 37 °C, 5% CO_2.

Melanoma cell lines

Four melanoma cell lines, commonly used in cytotoxicity studies, were purchased from ATCC (ATCC-LGC Standards GmbH, GERMANY). One wild-type for BRAF (SK-MEL-2), two homozygotes for BRAF p.Val600Glu (V600E); c.1799T > A (A375 and SK-MEL-28) and one heterozygote for the BRAF p.Val600Glu (MW-164).[47] The SK-MEL-2 genotype is also characterized as wild type for the genes CDK4, CDKN2A, and EGFR and homozygous for NRAS.Gln61Arg (c.182 A > G): The SK-MEL-28 genotype is also being characterized as wild-type for the NRAS and CDKN2 A genes, heterozygous for CDK4 p.Arg24Cys (c.70 C > T) and homozygous for EGFR p.Pro753Ser (c.2257 C > T). The latter mutation is classified as a possible pathogenic and found in squamous cell carcinomas sensitive to cetuximab (EGFR inhibitor).[37] The A375 genotype is also being characterized as wild-type for N-RAS, CDK4, and EGFR genes; however, multiple nonsense mutations occur within the CDKN2 A gene (p.Glu61Ter (c.181G > T); p.Glu69Ter (c.205G > T)). The WM-164 is wild-type for all the genes mentioned above.

The SK-MEL-2 and SK-MEL-28 cell lines were grown in EMEM (Earle's minimal essential medium) nutrient, containing non-essential amino acids, 2 mM L-glutamine, and 1 mM sodium pyruvate and 1500 mg/L sodium bicarbonate with 10% FBS and 1% penicillin/streptomycin solution. Cell lines A375 and WM-164 were grown in a medium containing DMEM (Dulbecco's Modified Eagle Medium), 10% FBS, and 1% penicillin/streptomycin solution. All cell cultures were left for the cells to adhere to in the plastic wells for 24 h before each treatment. The incubator was set to a constant temperature of 37 °C and a CO_2 concentration of 5%.

Cell viability assays

Colorectal cancer cell lines

Cell viability was estimated with the Sulforhodamine assay. Cells were seeded for 24 h into 96-well microtiter plates. After completion of the treatment, fixation was performed with 10% trichloroacetic acid and staining with 0,4% SRB in 1% acetic acid. Absorbance was measured using a TECAN microplate reader (Safire II TECAN, Mannedorf, Switzerland) and cell viability was estimated.

Melanoma cell lines

The viability of the cells exposed to the different concentrations of the synthesized compounds using the MTT assay as previously described.[48] Briefly, cells were plated in 96-well plates (1×10^4 cells/well) and treated with concentrations of the synthesized compounds ranging from 1 μM to 100 μM for 72 h. DMSO-treated cells (0.1% DMSO) were also used to determine the solvent's potential interferences with the obtained results. The product of the reduction of MTT by mitochondria of viable proliferating cells, the insoluble colored formazan, was then dissolved in SDS (10%) and measured spectrophotometrically at a wavelength of 550 nm and background at 690 nm using the above mentioned TECAN microplate reader. All assays were carried out in quadruplicates, and at least two independent experiments were performed for each condition.

Viability statistical analysis

Sulforhodamine assay IC_{50} values were calculated using the GraphPad8 software. t-Test using the Sigmaplot 14.0 (Systat Software Inc, USA) was used for cell viability comparisons. When applicable, the half-maximal inhibitory concentrations (IC_{50}) were obtained using the Probit regression.[49]

Western blotting

Western blotting was performed in colorectal cancer cell lysates. Whole cell protein lysates were extracted with lysis buffer containing protease inhibitors, separated in an SDS-PAGE and transferred to a nitrocellulose membrane (Amersham, UK) as described previously.[50] Membranes were then incubated overnight with specific antibodies at 4 °C, washed with TBS-Tween20 and incubated with the proper secondary antibody for 1 h, at room temperature. The antibodies used were directed against p-ERK1/2 (sc-7383-Santa Cruz Biotechnology, Inc., Dallas, TX, USA). The secondary antibodies used were mouse anti-rabbit IgG-HRP (sc-2357) and goat anti-mouse IgG-HRP (sc-2005) (both from Santa Cruz Biotechnology, Inc., Dallas, TX, USA). The antibody signal was enhanced with chemiluminescence and captured on X-ray film Super RX–N (Fujifilm Tokyo, Japan). Values were measured using Studio Lite software (LI–COR Biotechnology, Lincoln, NE, USA) and levels were normalized against housekeeping proteins (GAPDH-sc-47724- Santa Cruz Biotechnology, Inc., Dallas, TX, USA). The blots presented are representative of 3, or more, independently repeated experiments.

Genome-wide mRNA quantitation

RNA extraction, reverse transcription

Colo-205 cancer cells were seeded in 6-well plates and left to attach overnight. Upon treatment, total RNA was extracted using the Trizol reagent (Ambion by Life Technologies, Foster City, CA, USA), followed by purification using Qiagen RNeasy kit with on-column DNase treatment according to the manufacturer's protocol (Qiagen, Venlo, Netherlands).

RNA sequencing and bioinformatics analysis

RNA sequencing (RNA-seq) was performed by BGI-Europe (Copenhagen, Denmark) on a DNBseq-G400 sequencing platform, as paired-end reads (100 bp, minimum 60,896,724 million reads). Quality control and trimming was performed with fastp v0.20.0.[51] Subsequently, STAR v2.7.3a[52] was used for the assembly and reads were aligned to the reference genome (Human genome GRCh38.p12, retrieved via Gencode). Sequence reads were assigned to genomic features (GRCh38.p12) with featureCounts (R package Rsubread/Bioconductor),[53] in R environment (R v3.6.2). Upon gene annotation and expression quantification low counts filtering was performed, excluding counts per million (CPM) less than 1, for at least 2 samples. Normalization and differential expression analysis was performed with edgeR.[54] For the differentially expressed gene (DEG) lists, the following cutoffs were applied: absolute log2 Fold Change (logFC) >0.5 and p-value <0.05. For the annotation, mapIds and org.Hs.eg.db, were employed, while unmapped Ensembl IDs were removed from the final lists. Functional analysis was performed utilizing the BioInfoMiner platform,[55] which exploits statistical and network analysis algorithms for the identification and ranking of the significantly altered pathways and their relevant genes, with a hypergeometric p-value threshold of 0.05. The data presented in this study have been deposited in ArrayExpress (accession number: E-MTAB-13097).

Supporting Information

Supporting information for this article contains detailed experimental procedures for compounds **2**–**6**, **9a**–**k**, **13**, **15** and **19a**–**d**, copies of NMR and HRMS spectra and HPLC analyses for the final products **20**–**30**, additional figures for viability in colorectal and melanoma cancer cell lines, a table with predicted ADME profile of benzothiazoles, and lists of differentially expressed genes after treatment of Colo-205 cells with compound **22**.

Acknowledgements

We acknowledge support of this work by the project "STHENOS-b: Targeted therapeutic approaches against degenerative diseases with special focus on cancer and ageing-optimisation of the targeted bioactive molecules'' (MIS 5002398), which is funded by the Operational Programme "Competitiveness, Entrepreneurship and Innovation" (NSRF2014–2020) and co-financed by Greece and the EU (European Regional Development Fund). Concerning a fellowship for Y. Batsi, «this research is co-financed by Greece and the European Union (European Social Fund-ESF) through the Operational Programme «Human Resources Development, Education and Lifelong Learning» in the context of the project "Strengthening Human Resources Research Potential via Doctorate Research" (MIS-5000432), implemented by the State Scholarships Foundation (IKY)». This work was further supported by the "Infrastructure for Preclinical and early-Phase Clinical Development of Drugs, Therapeutics and Biomedical Devices (EATRIS-GR)" (MIS 5028091), which is implemented under the Action "Reinforcement of the Research and Innovation Infrastructure", funded by the Operational Programme "Competitiveness, Entrepreneurship and Innovation" (NSRF2014–2020) and co-financed by Greece and the European Union (European Regional Development Fund). We also thank Eleni Siapi for HRMS measurements.

Conflict of Interests

The authors declare no conflict of interest.

Data Availability Statement

The data that support the findings of this study are available in the supplementary material of this article.

Keywords: Benzothiazole · BRAFV600E inhibitors · *In silico* studies · *In vitro* biological evaluation · Cancer

[1] A. Zambon, D. Niculescu-Duvaz, I. Niculescu-Duvaz, R. Marais, C.J Springer, *Expert Opin. Ther. Pat.* **2013**, *23*, 155–164.
[2] M. A. Rahman, A. Salajegheh, R. A. Smith, A. K.-Y. Lam, *Crit. Rev. Oncol. Hematol.* **2014**, *90*, 220–232.
[3] P. M. Fischer, *Med. Res. Rev.* **2017**, *37* 314–367.
[4] L. Santarpia, S. M. Lippman, A. K. El-Naggar, *Expert Opin. Ther. Targets* **2012**, *16*, 103–119.
[5] A. K. Freeman, D. A. Ritt, D. K. Morrison, *Small GTPases* **2013**, *43*, 180–185.
[6] T. Amaral, T. Sinnberg, F. Meier, C. Krepler, M. Levesque, H. Niessner, C. Garbe, *Eur. J. Cancer* **2017**, *73*, 85–92.
[7] H. B. El-Nassan, *Eur. J. Med. Chem.* **2014**, *72*, 170–205.
[8] B. Agianian, E. Gavathiotis, *J. Med. Chem.* **2018**, *61*, 5775–5793.
[9] A. A. Samatar, P. I. Poulikakos, *Nat. Rev. Drug Discovery* **2014**, *13*, 928–942.
[10] A. Djanani, S. Eller, D. Öfne, J. Troppmair, M. Maglione, *Int. J. Mol. Sci.* **2020**, *21*, 9001.
[11] V. Subbiah, C. Baik, J. M. Kirkwood, *Trends Cancer* **2020**, *6*, 797–810.
[12] P. Lito, N. Rosen, D. B. Solit, *Nat. Med.* **2013**, *19*, 1401–1409.
[13] S. Sloot, I.V Fedorenko, K.SM. Smalley, G.T Gibney, *Expert Opin. Pharmacother.* **2014**, *15*, 589–592.
[14] C. Zhang, W. Spevak, Y. Zhang, E. A. Burton, Y. Ma, G. Habets, J. Zhang, J. Lin, T. Ewing, B. Matusow, G. Tsang, A. Marimuthu, H. Cho, G. Wu, W. Wang, D. Fong, H. Nguyen, S. Shi, P. Womack, M. Nespi, R. Shellooe, H. Carias, B. Powell, E. Light, L. Sanftner, J. Walters, J. Tsai, B. L. West, G. Visor, H. Rezaei, P. S. Lin, K. Nolop, P. N. Ibrahim, P. Hirth, G. Bollag, *Nature* **2015**, *526*, 583–586.
[15] R. Dummer, A. Hauschild, N. Lindenblatt, G. Pentheroudakis, U. Keilholz, *Ann. Oncol.* **2015**, *26*, 126–132.
[16] R. Roskoski Jr., *Pharmacol. Res.* **2017**, *117*, 20–31.
[17] V. Subbiah, C. Baik, J. M. Kirkwood, *Trends Cancer* **2020**, *6*, 797–810.
[18] C. Robert, B. Karaszewska, J. Schachter, P. Rutkowski, A. Mackiewicz, D. Stroiakovski, M. Lichinitser, R. Dummer, F. Grange, L. Mortier, V. Chiarion-Sileni, K. Drucis, I. Krajsova, A. Hauschild, P. Lorigan, P. Wolter, G. V. Long, K. Flaherty, P. Nathan, A. Ribas, A.-M. Martin, P. Sun, W. Crist, J. Legos, S. D. Rubin, S. M. Little, D. Schadendorf, *N. Engl. J. Med.* **2015**, *372*, 30–39.
[19] R. Dummer, P. A. Ascierto, H. J. Gogas, A. Arance, M. Mandala, G. Liszkay, C. Garbe, Di. Schadendorf, I. Krajsova, R. Gutzmer, V. Chiarion-Sileni, C. Dutriaux, J. W. B. de Groot, N. Yamazaki, C. Loquai, L. A. Moutouh-de Parseval, M. D. Pickard, V. Sandor, C. Robert, K. T. Flaherty, *Lancet Oncol.* **2018**, *19*, 603–615.
[20] J. Larkin, P. A. Ascierto, B. Dréno, V. Atkinson, G. Liszkay, M. Maio, M. Mandalà, L. Demidov, D. Stroyakovskiy, L. Thomas, L. de la Cruz-Merino, C. Dutriaux, C. Garbe, M. A. Sovak, I. Chang, N. Choong, S. P. Hack, G. A. McArthur, A. Ribas, *N. Engl. J. Med.* **2014**, *371*, 1867–1876.
[21] A. Rossi, M. Roberto, M. Panebianco, A. Botticelli, F. Mazzuca, P. Marchetti, *Eur. J. Pharmacol.* **2019**, *862*, 1726212.
[22] G. V. Long, K. T. Flaherty, D. Stroyakovskiy, H. Gogas, E. Levchenko, F. de Braud, J. Larkin, C. Garbe, T. Jouary, A. Hauschild, V. Chiarion-Sileni,

C. Lebbe, M. Mandalà, M. Millward, A. Arance, I. Bondarenko, J. B. A. G. Haanen, J. Hansson, J. Utikal, V. Ferraresi, P. Mohr, V. Probachai, D. Schadendorf, P. Nathan, C. Robert, A. Ribas, M. A. Davies, S. R. Lane, J. J. Legos, B. Mookerjee, J.-J. Grob, *Ann. Oncol.* **2017**, *28*, 1631–1639.
[23] "FDA approves atezolizumab for BRAF V600 unresectable or metastatic melanoma", can be found under http://www.fda.gov/drugs/resources-information-approved-drugs/fda-approves-atezolizumab-braf-v600-unresectable-or-metastatic-melanoma (accessed 15 November 2021).
[24] K. Koumaki, G. Kontogianni, V. Kosmidou, F. Pahitsa, E. Kritsi, M. Zervou, A. Chatziioannou, V. L. Souliotis, O. Papadodima, A. Pintzas, *Biochim. Biophys. Acta Mol. Basis Dis.* **2021**, *1867*, 166061.
[25] Z. Yao, Y. Gao, W. Su, R. Yaeger, J. Tao, N. Na, Y. Zhang, C. Zhang, A. Rymar, A. Tao, N. M. Timaul, R. Mcgriskin, N. A. Outmezguine, H. Y. Zhao, Q. Chang, B. Qeriqi, M. Barbacid, E. de Stanchina, D. M. Hyman, G. Bollag, N. Rosen, *Nat. Med.* **2019**, *25*, 284–291.
[26] It was prepared as described in the following paper, in which however, the NMR data is absent: H. He, H. Xia, Q. Xia, Y. Ren, H. He, *Bioorg. Med. Chem.* **2017**, *25*, 5652–5661.
[27] It was prepared as described in the following paper, in which however, the NMR data is absent: F. Lo Monte, T. Kramer, J. Gu, M. Brodrecht, J. Pilakowski, A. Fuertes, J. M. Dominguez, B. Plotkin, H. Eldar-Finkelman, B. Schmidt, *Eur. J. Med. Chem.* **2013**, *61*, 26–40.
[28] It was prepared as previously reported: J. Tan, W. Tang, Y. Sun, Z. Jiang, F. Chen, L. Xu, Q. Fan, J. Xiao, *Tetrahedron* **2011**, *67*, 6206–6213.
[29] It was prepared by a modified procedure to that previously reported: M. Ankersen, M. Crider, S. Liu, B. Ho, H. S. Andersen, C. Stidsen, *J. Am. Chem. Soc.* **1998**, *120*, 1368–1373.
[30] It was prepared as previously reported: X. Zha, L. Wu, S. Xu, F. Zou, J. Xi, T. Ma, R. Liu, Y–C. Liu, D. Deng, Y. Gu, J. Zhou, F. Lan, *Med. Chem. Res.* **2016**, *25*, 2822–2831.
[31] It was prepared as previously reported: Y–Y. Chu-Farseeva, N. Mustafa, A. Poulsen, E. C. Tan, J. Y. Yen, W. J. Chng, B. W. Dymock, *Eur. J. of Med. Chem.* **2018**, *158*, 593–619.
[32] It was prepared as previously reported: M. Kajino, A. Hasuoka, N. Tarui, T. Takagi (TAKEDA PHARMACEUTICAL COMP. LTD.), EP1803709 A1, **2007**.
[33] It was prepared as previously reported: A. Le Pera, A. Leggio, A. Liguori, *Tetrahedron* **2006**, *62*, 6100–6106.
[34] It was prepared as previously reported: M. A. Dea-Ayuela, E. Castillo, M. Gonzalez-Alvarez, C. Vega, M. Rolón, F. Bolás-Fernández, J. Borrás, M. E. González-Rosende, *Bioorg. Med. Chem.* **2009**, *17*, 7449–7456.
[35] It was prepared as described in the following patent, in which however, the NMR data is absent: L. Feng, M. Huang, Y. Liu, G. Wu, S. Yan, H. Yun, M. Zhou, US2012/0190677 A1, **2012**.
[36] It was prepared by a modified procedure to that previously reported: V. Palchykov, N. Manko, N. Finiuk, R. Stoika, M. Obushak, N. Pokhodylo, *Med. Chem. Res.* **2022**, *31*, 284–292.
[37] P. Ganesan, S. M. Ali, K. Wang, G. R. Blumenschein, B. Esmaeli, R. A. Wolff, V. A. Miller, P. J. Stephens, J. S. Ross, G. A. Palmer, F. Janku, *J. Clin. Oncol.* **2016**, *34*, 34–37.
[38] E. Lomonosova, G. Chinnadurai, *Oncogene* **2008**, *27*, S2–S19.
[39] C. L. Armstrong, R. Galisteo, S. A. N. Brown, J. A. Winkles, *Oncotarget.* **2016**, *7*, 81474–81492.
[40] Schrödinger Release 2020–3: LigPrep, Schrödinger, LLC, New York, NY, **2020**.
[41] Schrödinger Release 2020–3: Maestro, Schrödinger, LLC, New York, NY, **2020**.
[42] Schrödinger Release 2020–3: Protein Preparation Wizard; Epik, Schrödinger, LLC, New York, NY, **2020**; Impact, Schrödinger, LLC, New York, NY; Prime, Schrödinger, LLC, New York, NY, **2020**.
[43] Schrödinger Release 202–3: Glide, Schrödinger, LLC, New York, NY, **2020**.
[44] Schrödinger Release 2020-3: QikProp, Schrödinger, LLC, New York, NY, **2020**.
[45] http://www.thermofisher.com/gr/en/home/products-and-services/services/custom-services/screening-and-profiling-services/selectscreen-profiling-service/selectscreen-kinase-profiling-service.html.
[46] G. Bollag, P. Hirth, J. Tsai, J. Zhang, P. N. Ibrahim, H. Cho, W. Spevak, C. Zhang, Y. Zhang, G. Habets, E. A. Burton, B. Wong, G. Tsang, B. L. West, B. Powell, R. Shellooe, A. Marimuthu, H. Nguyen, K. Y. J. Zhang, D. R. Artis, J. Schlessinger, F. Su, B. Higgins, R. Iyer, K. D'Andrea, A. Koehler, M. Stumm, P. S. Lin, R. J. Lee, J. Grippo, I. Puzanov, K. B. Kim, A. Ribas, G. A. McArthur, J. A. Sosman, P. B. Chapman, K. T. Flaherty, X. Xu, K. L. Nathanson, K. Nolop, *Nature* **2010**, *467*, 596–599.
[47] https://web.expasy.org/cellosaurus/.
[48] M.-S. Vidali, S. Dailianis, D. Vlastos, P. Georgiadis, *Environ. Toxicol. Pharmacol.* **2021**, *87*, 103696.
[49] D. J. Finney, *Probit Analysis: a statistical treatment of the sigmoid response curve*, Cambridge University Press, London, Reissue edition, July 20, **2009**.
[50] E. Oikonomou, M. Koc, V. Sourkova, L. Andera, A. Pintzas, *PLoS One* **2011**, *6*, 21632.
[51] S. Chen, Y. Zhou, Y. Chen, J. Gu, *Bioinformatics* **2018**, *34*, i884–i890.
[52] A. Dobin, C. A. Davis, F. Schlesinger, J. Drenkow, C. Zaleski, S. Jha, P. Batut, M. Chaisson, T. R. Gingeras, *Bioinformatics* **2013**, *29*, 15–21.
[53] Y. Liao, G. K. Smyth, W. Shi, *Bioinformatics* **2014**, *30*, 923–30.
[54] M. D. Robinson, D. J. McCarthy, G. K. Smyth, *Bioinformatics* **2010**, *26*, 139–40.
[55] T. Koutsandreas, I. Binenbaum, E. Pilalis, I. Valavanis, O. Papadodima, A. Chatziioannou, *Int. J. Monit. Surveill. Technol. Res.* **2016**, *4*, 30–49.

Manuscript received: June 23, 2023
Revised manuscript received: October 2, 2023
Accepted manuscript online: October 4, 2023
Version of record online: October 24, 2023